Measurement of the Neutron Electric Form Factor G_E^n in ${}^2\overrightarrow{\mathrm{H}}(\overrightarrow{e}, e'n)p$ Quasi-elastic Scattering

Donal Day
University of Virginia
Charlottesville, VA 22904
dbd@virginia.edu

March, 28, 2003

Plan

Nucleon Form Factors

$$\frac{d\sigma}{d\Omega} = \sigma_{\mathrm{Mott}} \frac{E'}{E_0} \left\{ (F_1)^2 + \tau \left[2 (F_1 + F_2)^2 \tan^2 (\theta_e) + (F_2)^2 \right] \right\}$$

$$\boxed{\begin{array}{ll} F_1^p = 1 & F_1^n = 0 \\ F_2^p = 1.79 & F_2^n = -1.91 \end{array}}$$

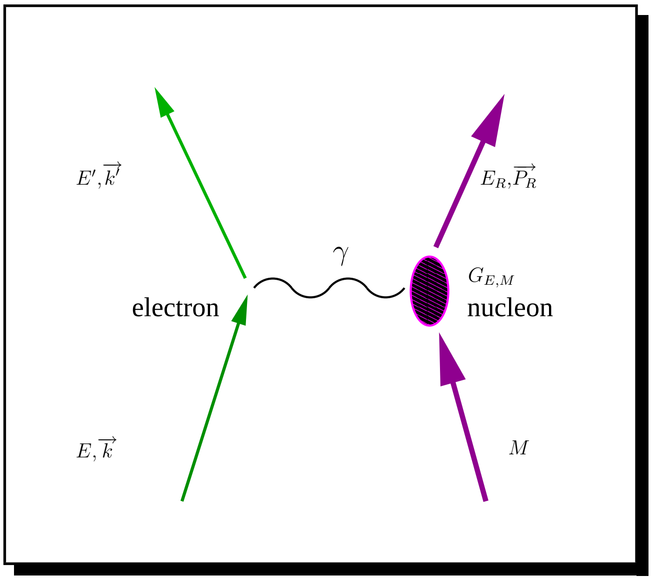

e scatt. angle: θ_e

pointlike target: $\sigma_{mott} = \frac{\alpha^2 \cos^2(\theta_e/2)}{4E^2 \sin^4(\theta_e/2)}$

Kin. factor: $\tau = Q^2/4M^2$

4-momentum transfer:

$$\begin{aligned} Q^2 &= \left(\overrightarrow{k} - \overrightarrow{k'} \right)^2 - (E - E')^2 \\ &= 4EE' \sin^2 (\theta_e/2) \end{aligned}$$

$$\boxed{G_E \left(Q^2\right) = F_1(Q^2) - \tau F_2 \left(Q^2\right) \quad G_M \left(Q^2\right) = F_1 \left(Q^2\right) + F_2 \left(Q^2\right)}$$

$$\frac{d\sigma}{d\Omega} = \frac{\sigma_{Mott}}{(1+\tau)} \frac{E'}{E_0} \left[G_E^2 + \tau (1 + (1+\tau) 2 \tan^2(\theta/2)) G_M^2 \right]$$

$Q^2 = 0$ limit: $G_E^p = 1$ $G_E^n = 0$ $G_M^p = 2.79$ $G_M^n = -1.91$

G_E^n Interpretation

In the nonrelativistic limit $Q^2 = \vec{q}^{\,2}$ (Breit Frame) G_E is Fourier Transform of the charge distribution $\rho(r)$:

$$
\begin{aligned}
G_E^n\left(\mathbf{q}^2\right) &= \frac{1}{(2\pi)^3}\int d^3r\rho(\mathbf{r})e^{(i\mathbf{q}\cdot\mathbf{r})} \\
&= \int d^3\mathbf{r}\rho\left(\mathbf{r}\right) - \frac{\mathbf{q}^2}{6}\int d^3\mathbf{r}\rho\left(\mathbf{r}\right)\mathbf{r}^2 + \ldots \\
&= 0 - \frac{\mathbf{q}^2}{6}\left\langle r_{ne}^2\right\rangle + \ldots
\end{aligned}
$$

Anomalous magnetic moment of neutron and Yukawa theory of mesons gave rise to the idea of a separated charge distribution in the neutron. The charge radius was expected to be negative.

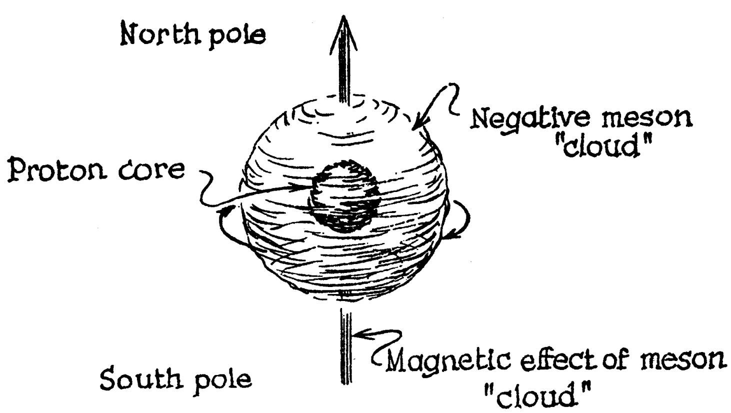

$$
\begin{aligned}
\left\langle r_{ne}^2\right\rangle = -6\frac{dG_E(0)}{dQ^2} &= -6\frac{dF_1(0)}{dQ^2} + \frac{3}{2M^2}F_2(0) \\
&= \left\langle r_{\text{in}}^2\right\rangle + \left\langle r_{\text{Foldy}}^2\right\rangle
\end{aligned}
$$

Charge radius, Foldy term

$$\left\langle r_{ne}^2 \right\rangle = -6\frac{dG_E^n(0)}{dQ^2} = -6\frac{dF_1^n(0)}{dQ^2} + \frac{3}{2M^2}F_2^n(0)$$
$$= \left\langle r_{\rm in}^2 \right\rangle + \left\langle r_{\rm Foldy}^2 \right\rangle$$

Foldy term, $\frac{3\mu_n}{2m_n} = (-0.126)\mathrm{fm}^2$, has nothing to do with the rest frame charge distribution.

$\left\langle r_{ne}^2 \right\rangle$ is measured through neutron-electron scattering

$$\left\langle r_{ne}^2 \right\rangle = \frac{3m_e a_0}{m_n} b_{ne} = -0.113 \pm 0.003 \pm 0.004\,\mathrm{fm}^2.$$

$\left\langle r_{\rm in}^2 \right\rangle = -0.113 + 0.126 \approx 0$ suggesting that the spatial charge extension seen in F_1 is about 0 or very small.

Recent studies have attempted to resolve this issue with the conclusion that G_E^n arises from the neutron's rest frame charge distribution.

N. Isgur Phys. Rev. Lett. 83, 272 (1999)

"Interpreting the Neutron's Electric Form Factor. Rest Frame Charge Distribution or Foldy Term?"

in relativistic expansion of the constituent quark model the Foldy term cancels against a contribution from F_1.

M. Bawin & A.A. Coon Phys. Rev. C. 60, 025207 (1999)

"Neutron charge radius and the Dirac equation"

explicit incorporation of the Dirac-Pauli form factors in Dirac equation. The Foldy term is canceled by a contribution from F_1.

Why is $\langle \mathbf{r}_{\mathrm{in}}^2 \rangle < 0$?

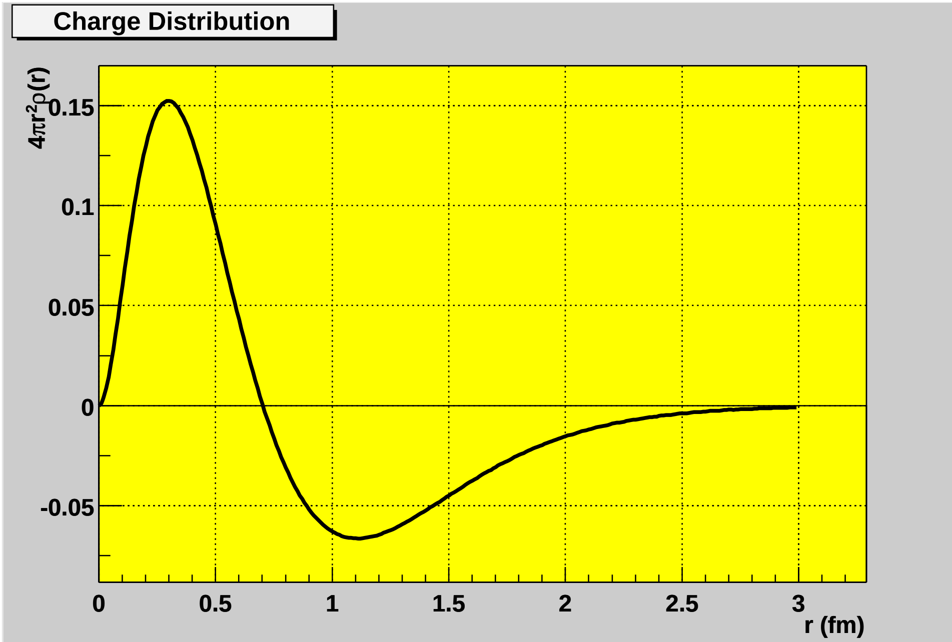

Hadron Picture

$p\pi^-$ component in neutron wavefunction

π^- cloud on outside

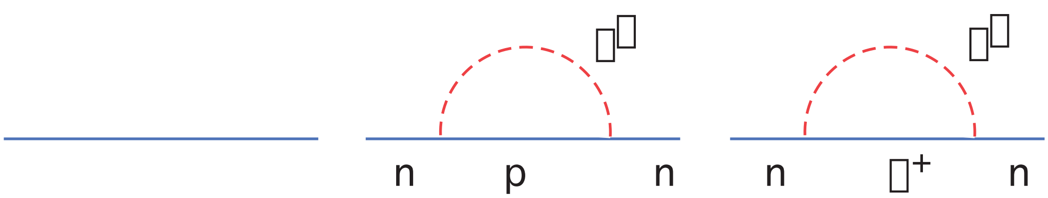

CQM

neutron $=$ udd and spin–spin forces create a charge segregation

Why measure $\mathrm{G_E^n}$?

Fundamental quantity

- Test of QCD description of the nucleon

  Symmetric quark model, with all valence quarks with same wavefunction, $G_E^n \equiv 0 \longrightarrow$ details of the wavefunctions

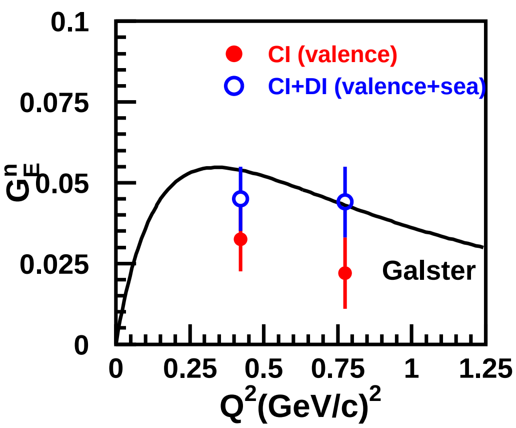

Dong, Liu, Williams, PRD 58 074504

- More sensitive than other form factors to sea quark contributions
- Soliton model *Gorski 1992* suggests that $\rho(r)$ at large r due to sea quarks

Necessary for study of nuclear structure.

- Without G_E^n almost impossible to extract information in high Q^2 few body structure functions
- Large source of error in extraction of strange quark form factors from parity violating experiments
- Explains $\langle \mathbf{r^2_{\mathrm{ch}}} \rangle$ of ^{48}Ca as compared to ^{40}Ca

Parametrizations of Nucleon Form Factors

The electric form factor, $G_E^p(Q^2) = \frac{1}{(2\pi)^3} \int d^3 r \rho(\mathbf{r}) e^{(i\mathbf{q}\cdot\mathbf{r})}$

Dipole Parametrization: Good description of early $G_{E,M}^p$ data

$$G_D = \left(1 + \frac{Q^2}{0.71(GeV/c)^2}\right)^{-2}$$

$$G_E^p = G_D = \frac{G_M^p}{\mu_p} = \frac{G_M^n}{\mu_n}$$

$$G_E^n = -\tau \mu_n G_D \, ; \ \tau = \frac{Q^2}{4M^2}$$

$G_D = \left(1 + \frac{Q^2}{k^2}\right)^{-2}$
implies an exponential charge distribution:
$\rho(r) \propto e^{-kr}$

Galster Parametrization: From $e - D$ elastic scattering

$$G_E^n = -\frac{\tau \mu_n}{1 + 5.6\tau} G_D$$

Models of Nucleon Form Factors

Ground state QCD structure is strong coupling problem: currently unsolvable

Vector Meson Dominance

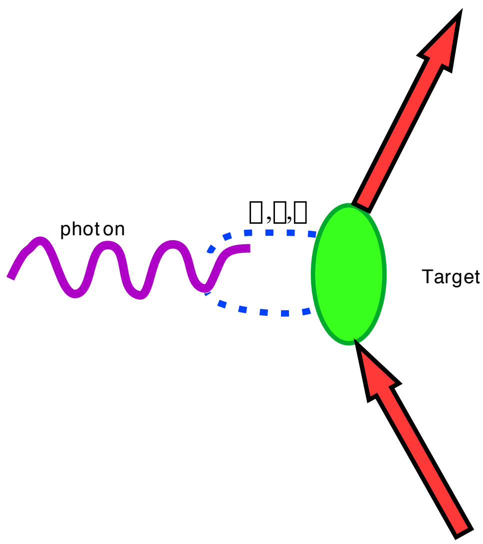

$$F(Q^2) = \sum_i \frac{C_{\gamma V_i}}{Q^2+M_{V_i}^2} F_{V_i N}(Q^2)$$

$\frac{1}{Q^2+M_{V_i}^2} \Rightarrow$ propagator of meson of mass M_{V_i}

$C_{\gamma V_i} \Rightarrow$ photon-meson coupling strength

$F_{V_i N}(Q^2) \Rightarrow$ meson-nucleon form factor.

VMD breaks down at large Q^2: Can not reproduce the dipole form factor or reproduce the prediction of pQCD.

pQCD

High Q^2 helicity conservation by $\gamma-$quark interaction requires that $Q^2F_1/F_2 \rightarrow$ constant as F_2 helicity flip arises from second order corrections and are suppressed by an additional factor of $1/Q$. Furthermore for $Q^2 \gg \Lambda_{QCD}$ counting rules find $F_1 \propto \alpha_s(Q^2)/Q^4$. Thus $F_1 \propto \frac{1}{Q^4}$ and $F_2 \propto \frac{1}{Q^6} \Rightarrow Q^2\frac{F_2}{F_1} \rightarrow$ constant. Contradicted by JLAB proton data which show that $Q\frac{F_2}{F_1} \rightarrow$ constant.

Hybrid Models

Failure to follow the high Q^2 behavior suggested by pQCD led GK to incorporate pQCD at high Q^2 with the low VMD behavior. Inclusion of ϕ by GK had significant effect on G_E^n. Lomon has updated with new fits to selected data.

Lattice calculations of form form factors nascent

Fundamental but currently limited in statistical accuracy

Dong *et al* PRD58, 074504 (1998)

QCD based modes

Models: try to capture aspects of QCD

RCQM P.L. Chung and F. Coester, PR D44, 229 (1991), I.Z. Aznaurian, PL B316, 39 (1993), M.R. Frank, B.K. Jennings, and G.A. Miller, PRC54, 920 (1996), M. Ivanov, M. Locher, and V. Lyubovitskij, Few Body Systems, 21, 131 (1996).

di-quark model P. Kroll, M.Schurmann, and W. Schweiger, Z. Phys. A432, 429 (1992).

QCD sum rules A.V. Radyushkin, Acta. Phys. Polon. B15, 403 (1984).

Cloudy bag model D.H. Lu, A.W. Thomas, and A.G. Williams, PR C57, 2628 (1998).

Helicity non-conservation shows up in the light front dynamics analysis of Miller and collaborators where in the imposition of Poincare invariance analytic results that predicted $Q\frac{F_2}{F_1} \longrightarrow$ constant and the violation of helicity conservation. Helicity non-conservation also shows up in the pQCD model of Ralston and collaborators which also predict that $Q\frac{F_2}{F_1} \longrightarrow$ constant. Both models include quark orbital angular momentum.

light front cloudy bag model Miller has extended the light front dynamics to include the cloudy bag with a description of the neutron as a bare nucleon and a negative pion cloud with a long tail, giving rise to the negative charge radius.

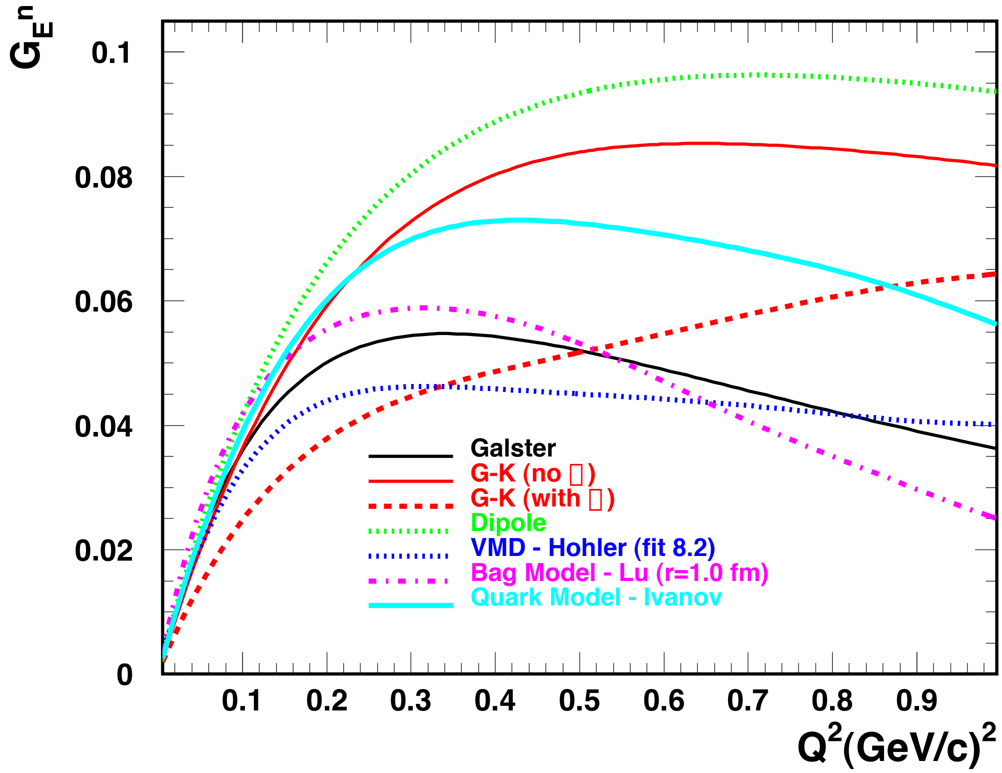

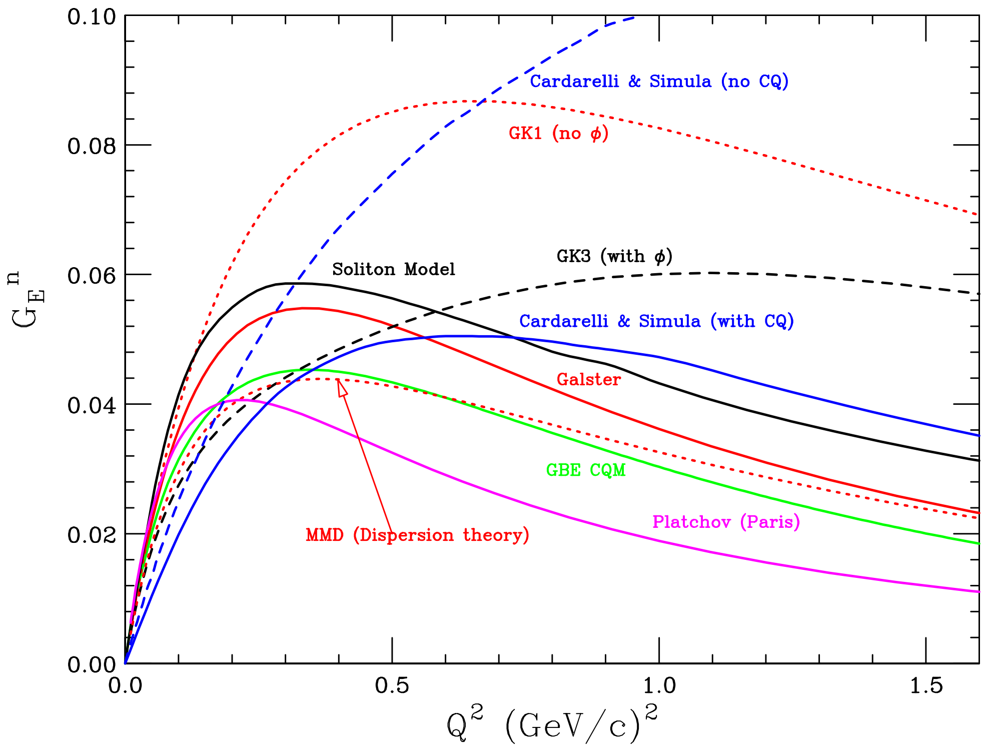

Soliton→Holzwarth MMD→ Mergell, Meissner and Dreschel
GBECQM→ Wagenbrum and collaborators

G_E^n Measurements

No free neutron target $\Longrightarrow$ Use deuteron

- Inclusive cross section measurements on Deuterium:
  - Elastic $e - D$ scattering at small angles:
    depends on N-N potential, subtraction of proton contribution
  - Quasielastic $e - D$ scattering
    Rosenbluth separation, sensitive to deuteron structure
- Double Polarization measurements
  asymmetry measurement
  detection of neutron in coincidence
  $\longrightarrow$ less sensitive to deutron structure
  $\longrightarrow$ avoid Rosenbluth separation
  $\longrightarrow$ avoid subtraction of proton contribution
  ${}^2\mathrm{H}(\overrightarrow{e}, e'\overrightarrow{n})p$, ${}^2\overrightarrow{\mathrm{H}}(\overrightarrow{e}, e'n)p$, ${}^3\overrightarrow{\mathrm{He}}(\overrightarrow{e}, e'n)pp$

Other methods

- ${}^2\mathrm{H}(e, e'n)p$
- ${}^2\mathrm{H}(e, e'\bar{\mathrm{p}})\mathrm{p}$ (anticoincidence)
- Ratio techniques$\frac{e,e'p}{e,e'n}$

e-D Elastic Scattering

Born approximation

$$\frac{d\sigma}{d\Omega} = \sigma_{NS}\left[A\left(Q^2\right) + B\left(Q^2\right)\tan^2\left(\frac{\theta_e}{2}\right)\right]$$

$$A(Q^2) = G_c^2 + \tfrac{8}{9}\eta G_Q^2 + \tfrac{2}{3}\eta^2 G_M^2$$
$$B(Q^2) = \tfrac{4}{3}\eta(\eta+1)G_M^2$$
$$\eta = \tfrac{Q^2}{4M_D^2}$$

small θ_e approximation

$$\frac{d\sigma}{d\Omega} = \cdots (G_e^p + G_E^n)^2 \left[u(r)^2 + w(r)^2\right] j_0(\frac{qr}{2})dr \cdots$$

1. $A_{IA}(Q^2)$ deduced after corrections for relativistic effects and MEC
2. Subtract magnetic dipole using parametrization of data
3. S and D state functions to unfold nuclear structure for various potentials to get isoscalar form factor
4. Subtract proton form factor
5. Sensitive to deuteron wavefunction model and MEC

Early measurements of G_E^n and slope at $Q^2 = 0$

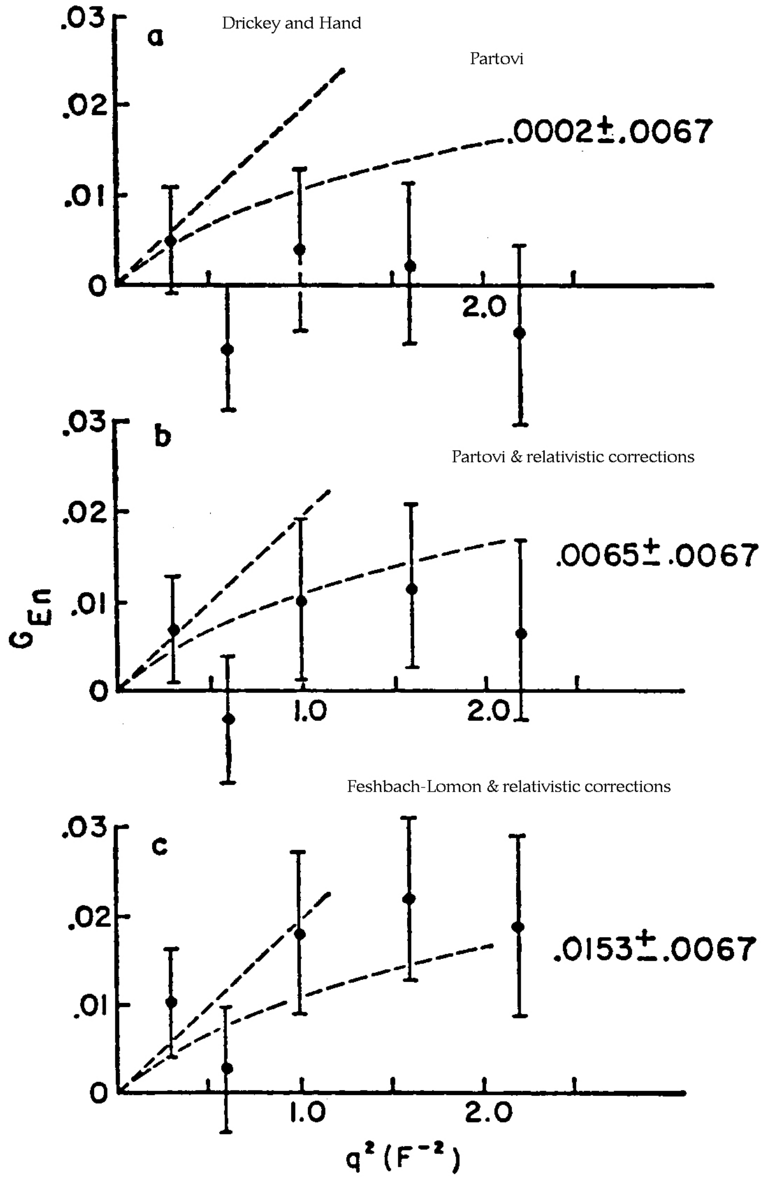

Relativistic corrections and model dependence: Casper and Gross, PR 155, 1607 (1967)

(a) Partovi wave function

(b) Partovi and relativistic corrections

(c) Feshbach-Lomon and relativistic corrections

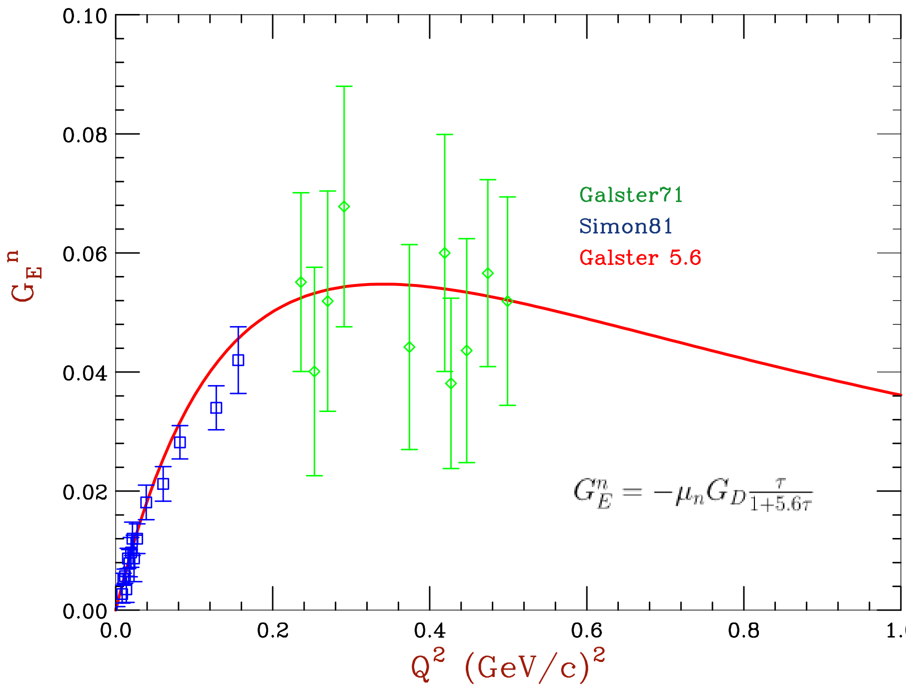
0.10
0.08
0.06
0.04
0.02
0.00
0.0
0.2
0.4
0.6
0.8
1.0
$G_E^{\,n}$
Q^2 (GeV/c)^2
Galster71
Simon81
Galster 5.6
$G_E^n = -\mu_n G_D \frac{\tau}{1+5.6\tau}$

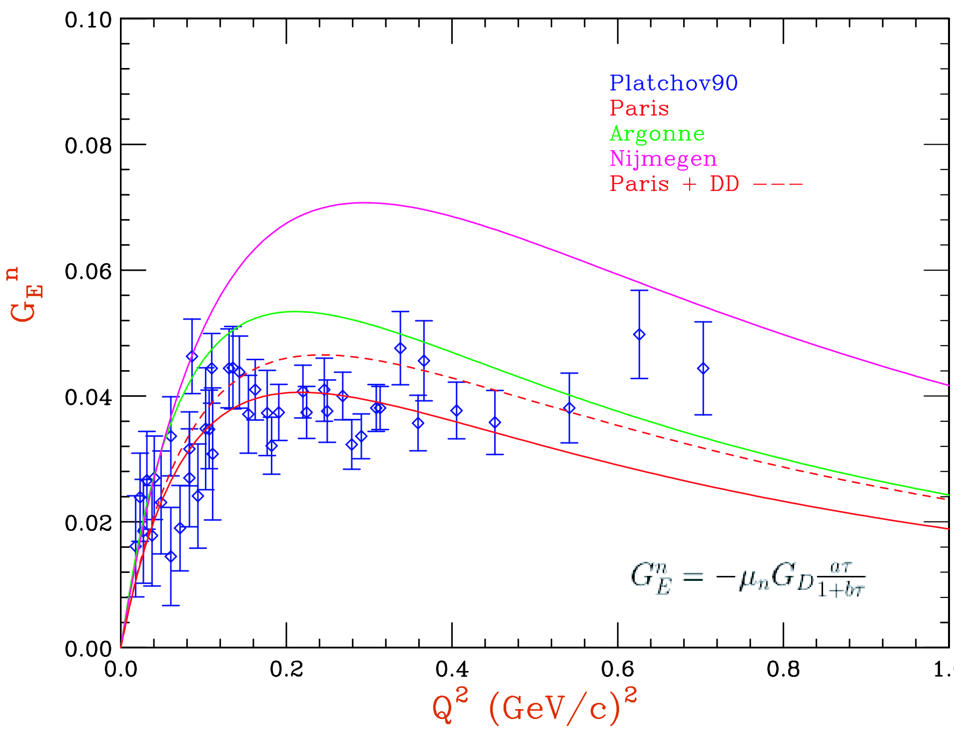
0.10
0.08
0.06
0.04
0.02
0.00
0.0
0.2
0.4
0.6
0.8
1.0
$G_E^{\,n}$
Q^2 (GeV/c)^2
Platchov90
Paris
Argonne
Nijmegen
Paris + DD ---
$G_E^n = -\mu_n G_D \frac{a\tau}{1+b\tau}$

Elastic, Continued

In the case of $^2\mathrm{H}(e,e')^2\overrightarrow{\mathrm{H}}$ components of the tensor polarization give useful combinations of the form factors,

$$t_{20} = \frac{1}{\sqrt{2}S}\left\{\frac{8}{3}\tau_d G_C G_Q + \frac{8}{9}\tau_d^2 G_Q^2 + \frac{1}{3}\tau_d\left[1+2(1+\tau_d)\tan^2(\theta/2)\right]G_M^2\right\}$$

allowing $G_Q(Q^2)$ to be extracted. Exploiting the fact that $G_Q(Q^2)$suffers less from theoretical uncertainties than $A(Q^2)$, G_E^n can be extracted to larger momentum transfers.

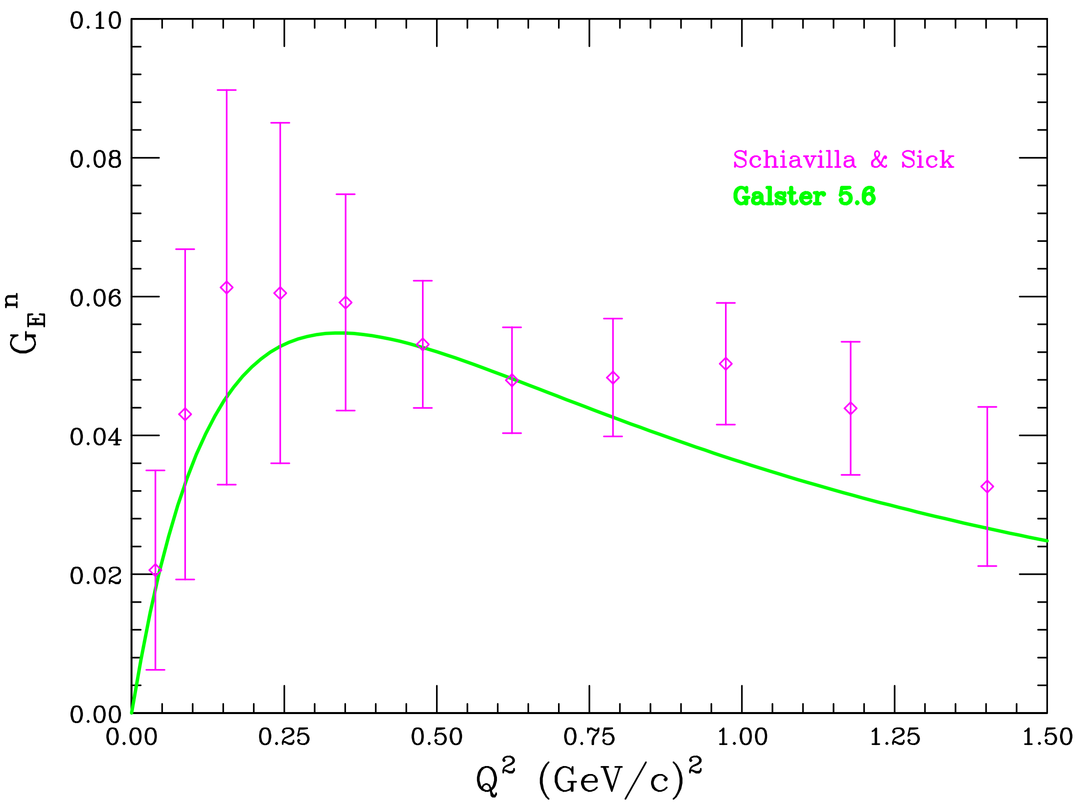

Quasielastic $e - d$ Scattering

PWIA model (Durand and McGee): Cross section is incoherent sum of p and n cross section folded with deuteron structure.

$$\begin{aligned}
\sigma &= (\sigma_p + \sigma_n)\, I(u,w) \\
&= \left\{ \varepsilon \left[\left(G_E^p\right)^2 + \left(G_E^n\right)^2 \right] + \frac{\nu^2}{Q^2} \left[\left(G_M^p\right)^2 + \left(G_M^n\right)^2 \right] \right\} I(u,w) \\
&= \varepsilon R_L + R_T \\
& \varepsilon = \left[1 + 2(1+\tau)\tan^2(\theta_e/2) \right]^{-1}
\end{aligned}$$

- Extraction of G_E^n:
  Rosenbluth Separation $\Rightarrow R_L$
  Subtraction of proton contribution
- Problems:
  Unfavorable error propagation
  Sensitivity to deuteron structure

SLAC: *A. Lung et al, Phys. Rev. Lett. 70, 718 (1993)*
$\rightarrow G_E^n$ consistent with zero and Galster.

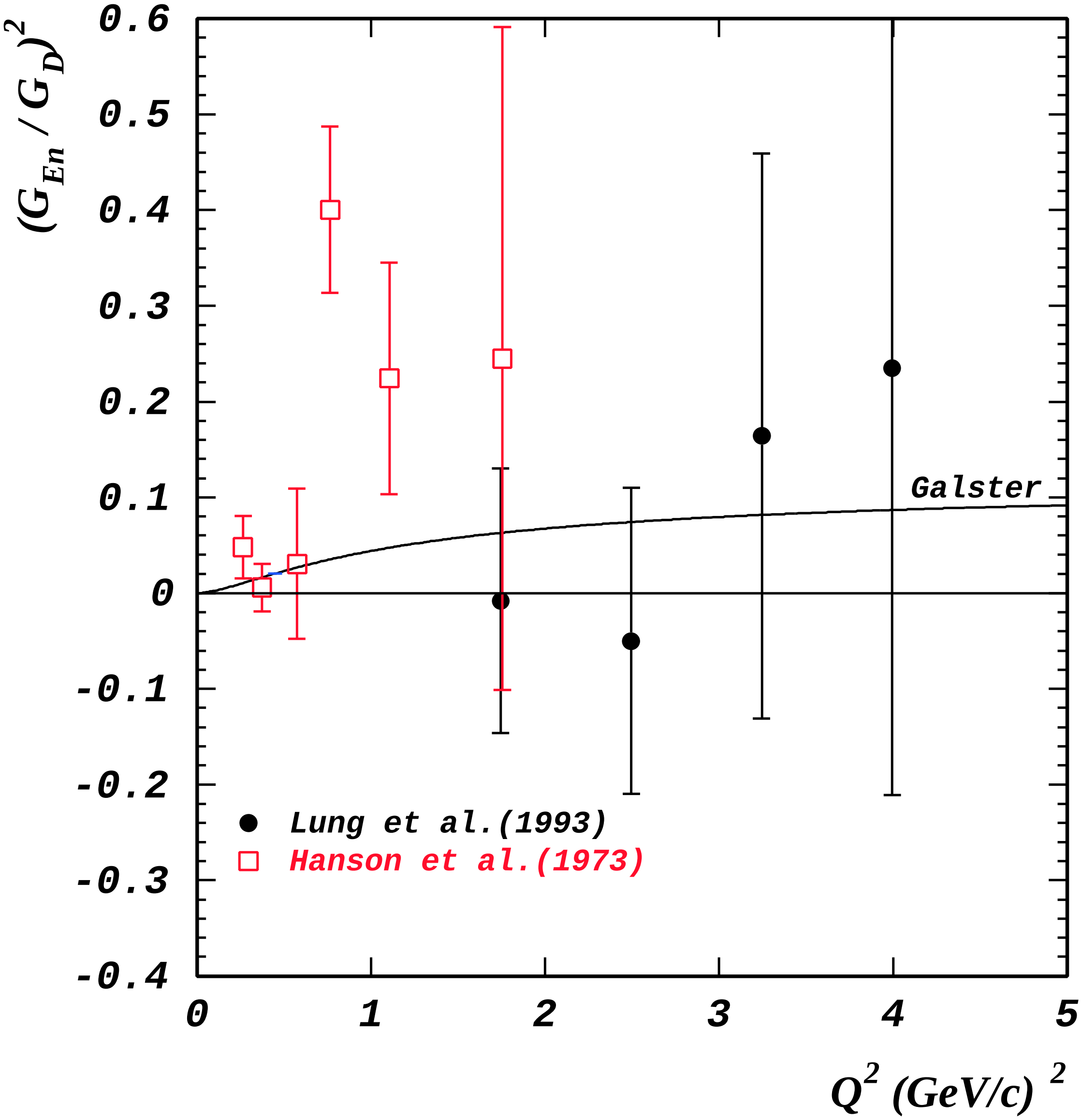

Open questions

$$\boxed{G_E\left(Q^2\right) = F_1(Q^2) - \tau F_2\left(Q^2\right) \quad G_M\left(Q^2\right) = F_1\left(Q^2\right) + F_2\left(Q^2\right)}$$

If G_E^n is small at large Q^2 then F_1^n must cancel τF_2^n, begging the question, how does F_1^n evolve from 0 at $Q^2 = 0$ to cancel τF_2^n at large Q^2?

E133 data from SLAC shows the ratio of σ_n/σ_p falling with Q^2, suggesting that

$F_1^n \simeq 0$. This implies that G_E^n would dominate G_M^n at high Q^2.

Double polarization measurements

Akhiezer and Rekalo (1968), Dombey (1968)

$^{2}\mathrm{H}(\vec{e}, e'\vec{n})p$

$^{2}\overrightarrow{\mathrm{H}}(\vec{e}, e'n)p$, $^{3}\overrightarrow{\mathrm{He}}(\vec{e}, e'n)pp$

Asymmetry measurements

$\longrightarrow$ less sensitive to deuteron structure

$\longrightarrow$ avoid Rosenbluth separation

$\longrightarrow$ avoid subtraction of proton contribution (detect neutron)

$\longrightarrow$ only relative charge measurement needed

$\longrightarrow$ reduced dependence on detector acceptance

$\longrightarrow$ radiative corrections reduced

$\longrightarrow$ understand helicity dependent deadtime

$\longrightarrow$ need absolute beam and target polarization

Target	Type	$Q^2(\mathrm{GeV/c})^2$	Reference
^{2}H	$(\vec{e}, e'\vec{n})$	0.15	C. Herberg *et al.*, Eur. Phys. J. A **5**, 131 (1999)
$^{2}\overrightarrow{\mathrm{H}}$	$(\vec{e}, e'n)$	0.21	I. Passchier *et al.*, Phys. Rev. Lett. **82**, 4988 (1999)
^{2}H	$(\vec{e}, e'\vec{n})$	0.252	T. Eden *et al.*, Phys. Rev. C **50**, R1749 (1994)
$^{3}\overrightarrow{\mathrm{He}}$	$(\vec{e}, e'n)$	0.31	M. Meyerhoff *et al.*, Phys. Lett. **B 327**, 201 (1994)
^{2}H	$(\vec{e}, e'\vec{n})$	0.33	M. Ostrick *et al.*, Phys. Rev. Lett. **83**, 276 (1999)
$^{3}\overrightarrow{\mathrm{He}}$	$(\vec{e}, e'n)$	0.36	J. Becker *et al.*, Eur. Phys. J . A**6**, 329 (1999)
$^{2}\overrightarrow{\mathrm{H}}$	$(\vec{e}, e'n)$	0.5	H. Zhu *et al.*, Phys. Rev. Lett. **87**, 081801 (2001)
$^{3}\overrightarrow{\mathrm{He}}$	$(\vec{e}, e'n)$	0.67	D. Rohe *et al.*, Phys. Rev. Lett. **83**, 4257 (1999)
$^{2}\overrightarrow{\mathrm{H}}$	$(\vec{e}, e'n)$	0.5, 1.0	JLAB E93-026 preliminary 2001
^{2}H	$(\vec{e}, e'\vec{n})$	0.45, 1.15, 1.47	JLAB E93-038 preliminary 2001
$^{3}\overrightarrow{\mathrm{He}}$	$(\vec{e}, e'n)$	0.67	Mainz 2003, Bermuth
^{2}H	$(\vec{e}, e'\vec{n})$	0..3, 0.6, 0.8	Mainz data taking completed 2002

Polarized Electron on Polarized Free Neutron

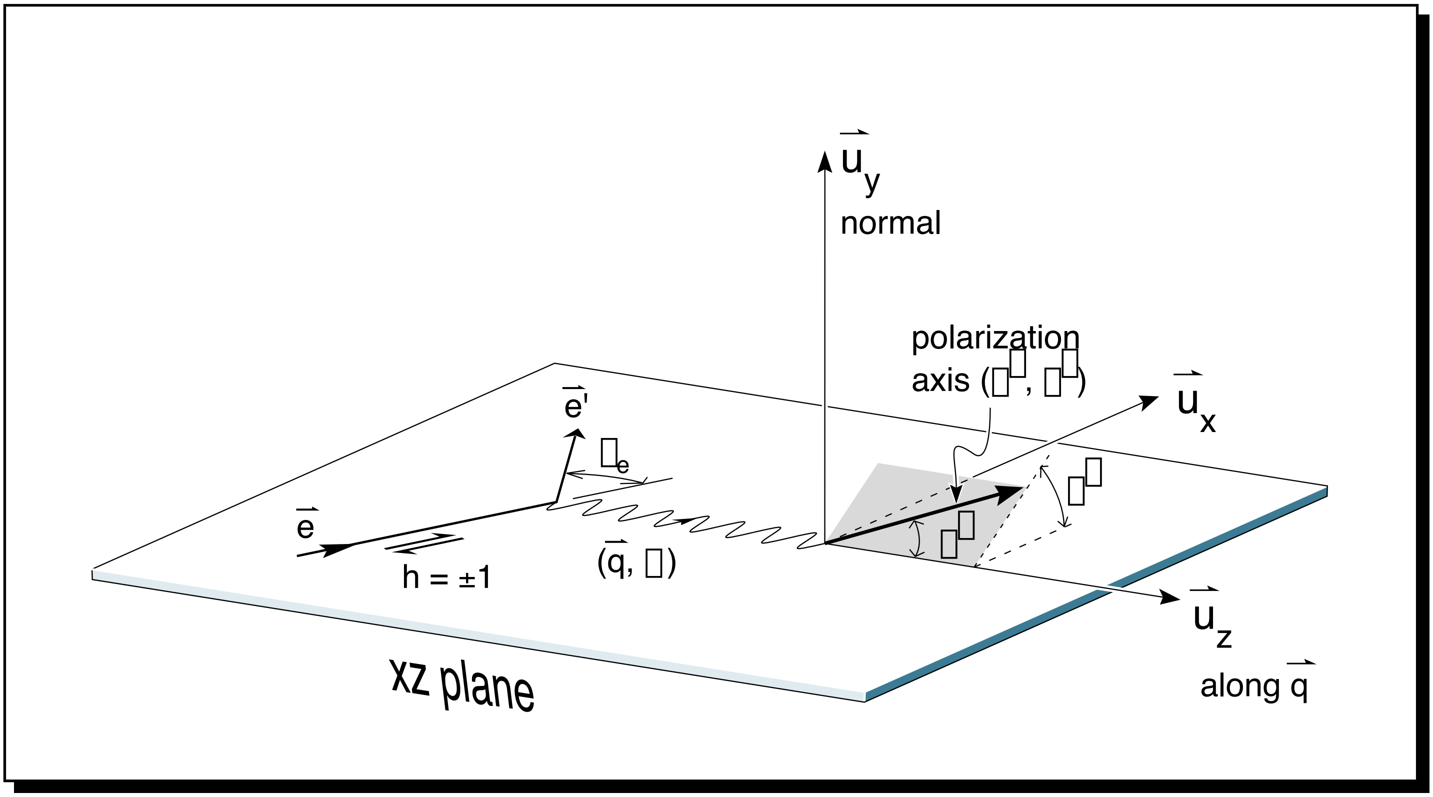

Neutron Polarization P Beam Helicity h

Polarized Cross Section: $\sigma = \sigma_0 \left(1 + hPA\right)$

$$A = \frac{a \cos\theta^{\star} \left(G_M^n\right)^2 + b \sin\theta^{\star} \cos\Phi^{\star} G_E^n G_M^n}{c \left(G_M^n\right)^2 + d \left(G_E^n\right)^2}$$

$$\theta^{\star} = 90^{\circ} \quad \Phi^{\star} = 0^{\circ} \implies A = \frac{b G_E^n G_M^n}{c \left(G_M^n\right)^2 + d \left(G_E^n\right)^2}$$

Polarized Electron on Polarized Deuteron Target

Polarized Cross Section for quasielastic $^2\overrightarrow{\mathrm{H}}(\overrightarrow{e}, e'n)p$:

$$\sigma(h,P) = \sigma_0 \left(1 + hA_e + PA_d^V + TA_d^T + hPA_{ed}^V + hTA_{ed}^T\right)$$

h: Beam Helicity

P: Vector Target Polarization

T: Tensor Target Polarization $T = 2 - \sqrt{4 - 3P^2}$

Deuteron supports a tensor polarization, T, in addition to the usual vector polarization, P – this can lead to both helicity dependent and helicity independent contributions

- A_{ed}^T and A_e vanish if symmetrically averaged
- A_d^V vanishes in the scattering plane
- A_d^T is suppressed by $T \approx 3\%$

Theoretical Calculations of electrodisintegration of the deuteron:

H. Arenhövel, W. Leidemann, and E. L. Tomusiak, Z. Phys. A 331, 123 (1988); 334, 363(E) (1989).

H. Arenhövel, W. Leidemann, and E. L. Tomusiak, Phys. Rev. C 46, 455 (1992).

A_{ed}^V is sensitive to G_E^n

has low sensitivity to potential models

has low sensitivity to subnuclear degrees of freedom (MEC, IC)

under certain kinematical conditions....

Sensitivity to G_E^n – Insensitivity to Reaction

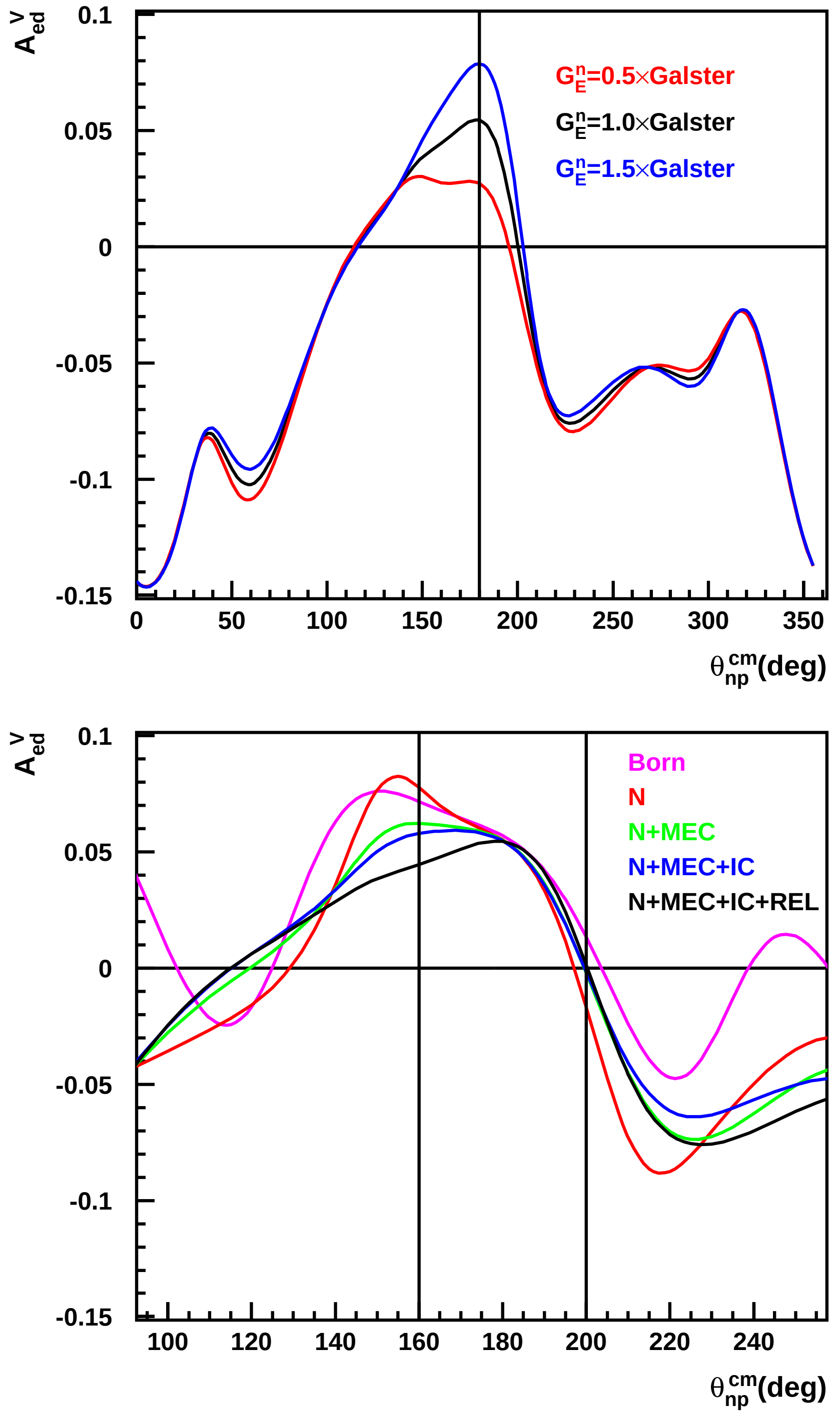

θ_{np}^{cm} : Angle between $\vec{q}$ and relative n-p momentum in cm system; 180 deg corresponds to neutron in direction of $\vec{q}$

Experimental Technique for ${}^2\overrightarrow{\mathrm{H}}(\overrightarrow{e}, e'n)p$

How to access A_{ed}^V?

Experiment measures counts for different orientations of h and P:

$$N^{hP} \propto \sigma\,(h, P)$$

Beam-target Asymmetry:

$$\begin{aligned} A_{BT} &= \frac{N^{++} - N^{-+} + N^{--} - N^{+-}}{N^{++} + N^{-+} + N^{++} + N^{++}} \\ &= \frac{hPA_{ed}^V}{1 + TA_d^T} \\ &\simeq hPA_{ed}^V \end{aligned}$$

E93026 Collaboration

112 collaborators from 18 institutions

Duke University, Florida International University,
Hampton University, Jefferson Lab, Louisiana Tech University,
Mississippi State University, Norfolk State University,
North Carolina A&T State University, Old Dominion University,
Ohio University, Southern University at New Orleans,
Tel Aviv University, University of Basel,
University of Maryland at College Park, University of Virginia,
Virginia Polytechnic Institute & State University,
Vrije Universiteit of Amsterdam, Yerevan Physics Institute

Experiment E93026

- Measured in Hall C at Thomas Jefferson National Accelerator Facility (Jlab) in Newport News, Virginia, USA
- Measuring periods
  - Aug 1998 - Oct 1998
  - July 2001 - Dec 2001
- Kinematics:

  2.2×10^6 neutrons at $Q^2 = 0.5$ (GeV/c)^2 (1998)
  6.5×10^6 neutrons at $Q^2 = 0.5$ (GeV/c)^2 (2001)
  $.75 \times 10^6$ neutrons at $Q^2 = 1.0$ (GeV/c)^2 (1998)
  1.4×10^6 neutrons at $Q^2 = 1.0$ (GeV/c)^2 (2001)

Hall Schematic

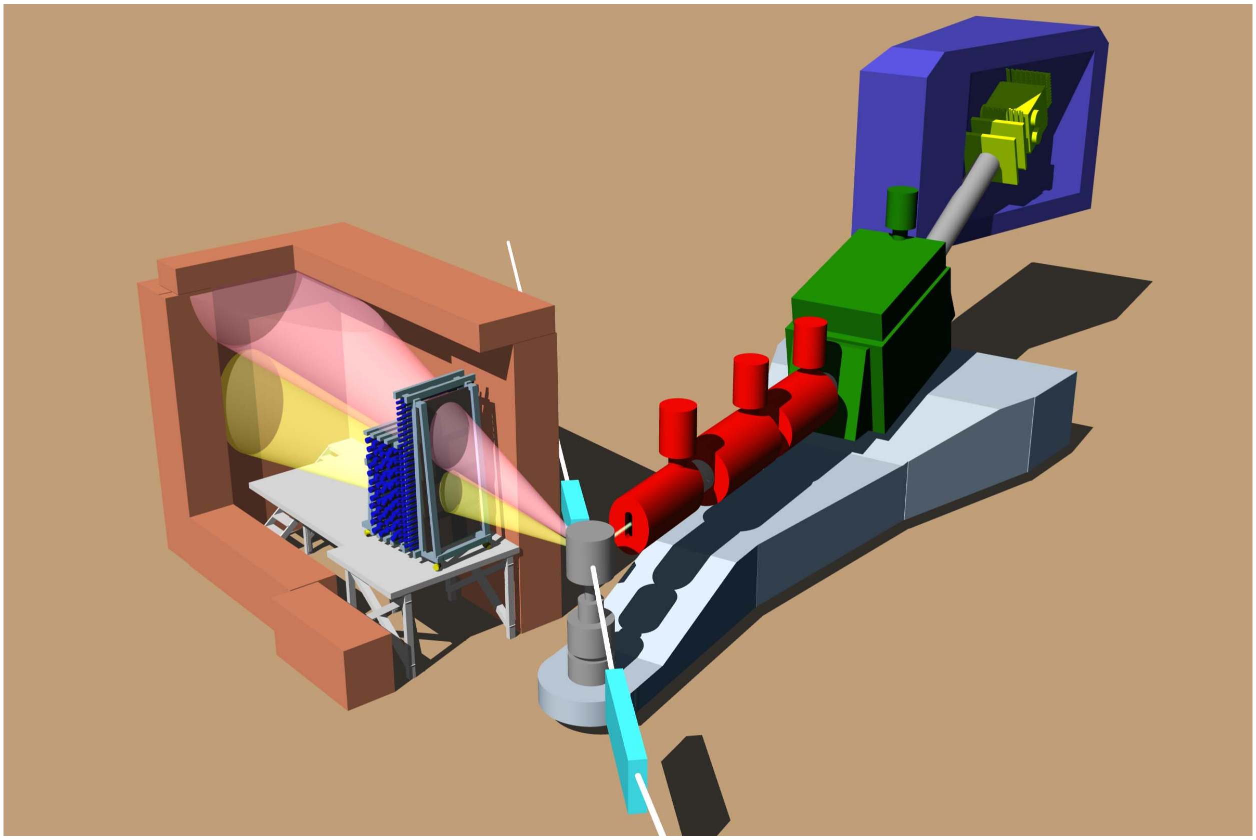

- Polarized Target
- Chicane to compensate for beam deflection of $\approx$ 4 degrees
- Scattering Plane Tilted
- Protons deflected $\approx$ 17 deg at $Q^2 = 0.5$
- Raster to distribute beam over 3 cm^2 face of target
- Electrons detected in HMS (right)
- Neutrons and Protons detected in scintillator array (left)
- Beam Polarization measured in coincidence Möller polarimeter

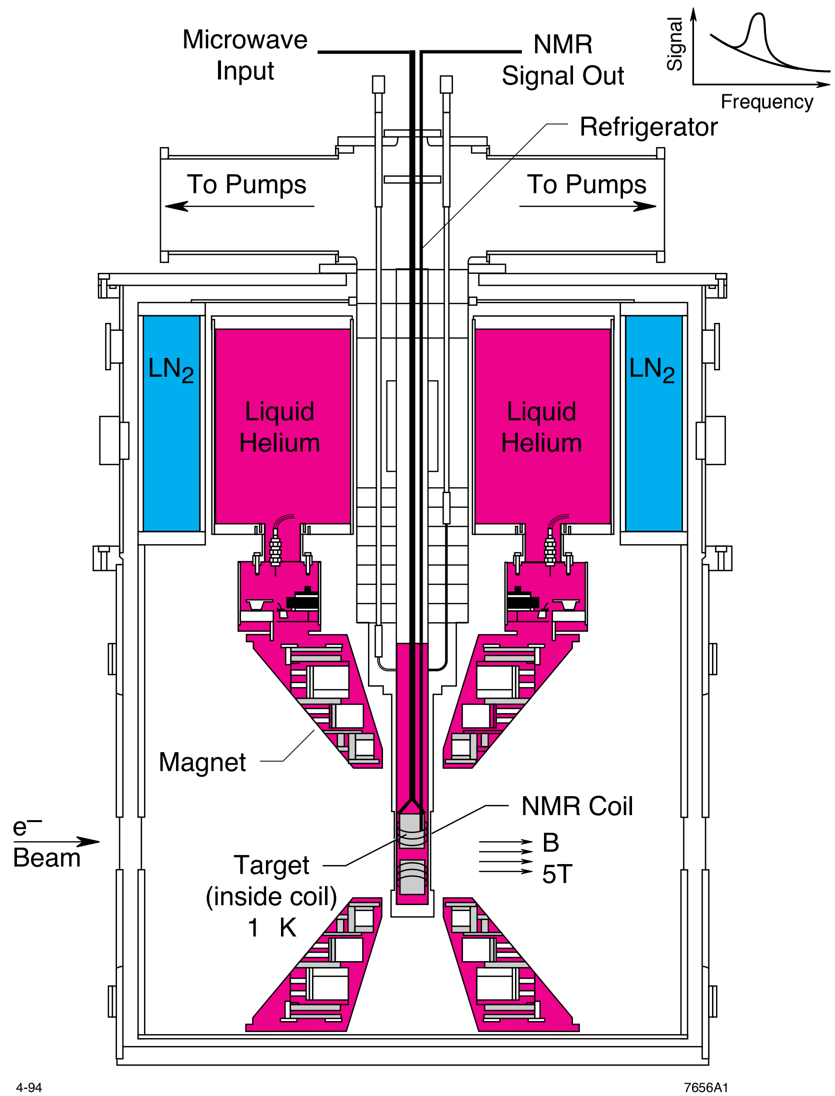

Solid Polarized Targets

- frozen(doped) $^{15}ND_3$
- ^{4}He evaporation refrigerator
- $5T$ polarizing field
- remotely movable insert
- dynamic nuclear polarization

Dynamic Nuclear Polarization

Pictorial Representation–Proton Enhancement

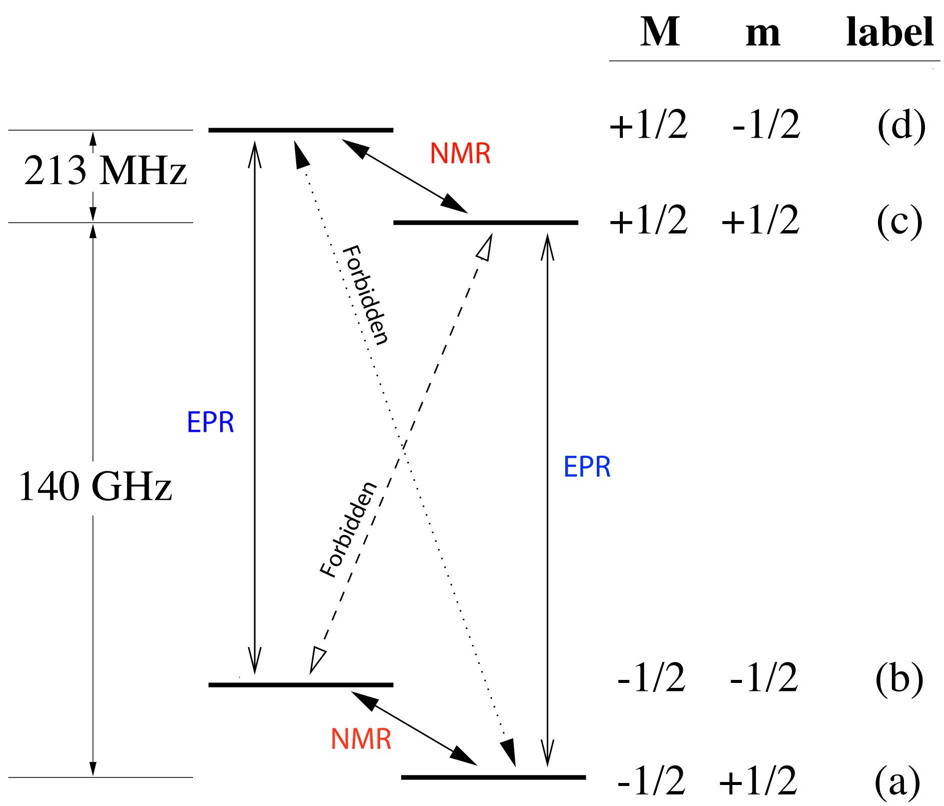

Forbidden transitions ($\Delta m_j \neq \pm 1$) allowed

Microwaves of 140Ghz - 213 MHz drive the $\mathbf{b} \rightarrow \mathbf{c}$ transition

Relaxation occurs through $\mathbf{c} \rightarrow \mathbf{a}$ transition

Target Stick

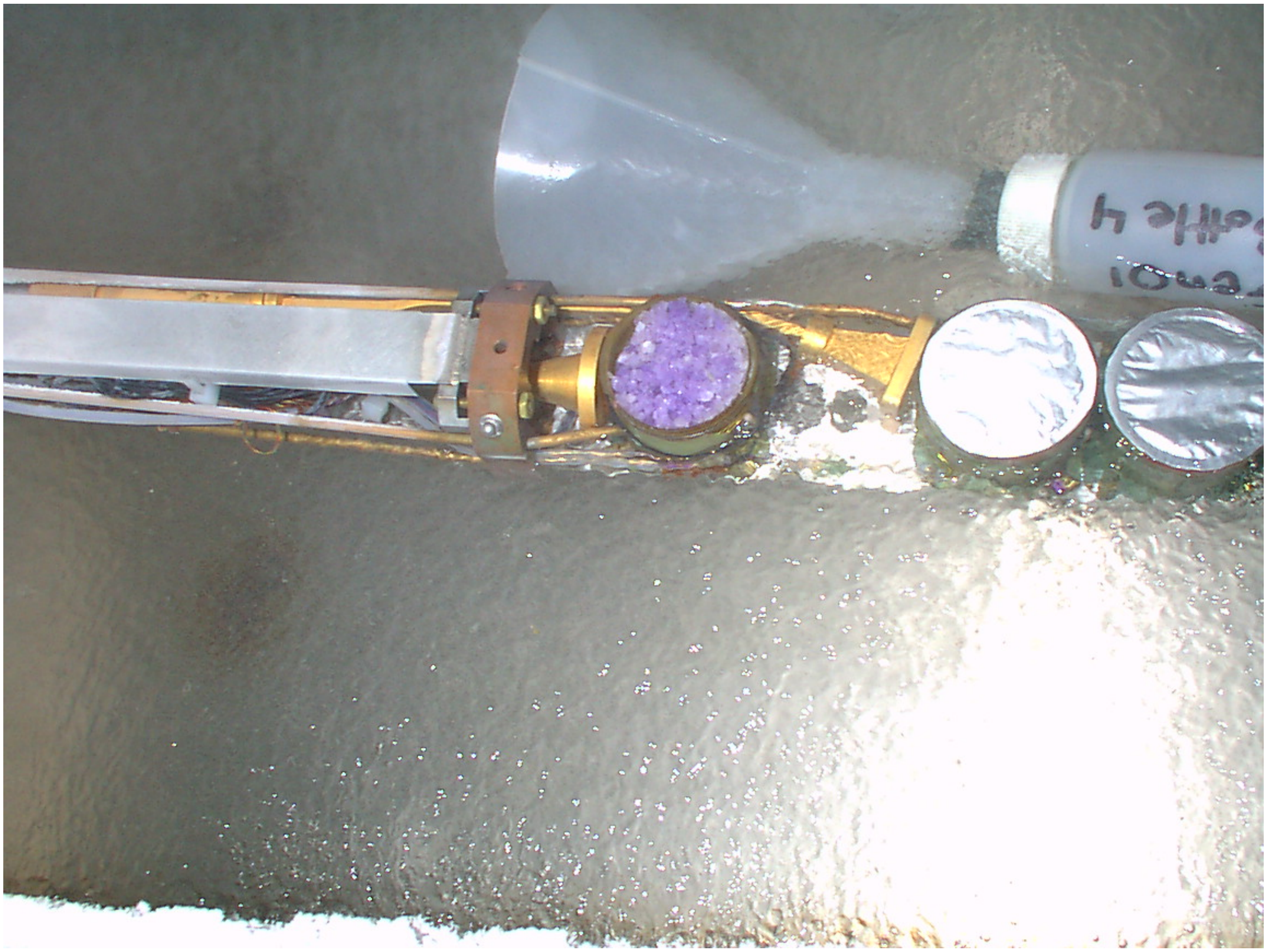

Deuteron NMR

- Sweep RF frequency-measure absorptive part of response with tuned phase sensitive circuit
- Polarization proportional to signal area
- Fix scale by measuring polarization in thermal equilibrium (TE) @ (5 Tesla, 1.5 K)

$$P_{\mathrm{TE}} = \frac{4\tanh(\mu B/2kT)}{3 + \tanh^2(\mu B/2kT)} \approx 0.07\%$$

Typically can achieve 3 to 5% systematic error (relative)

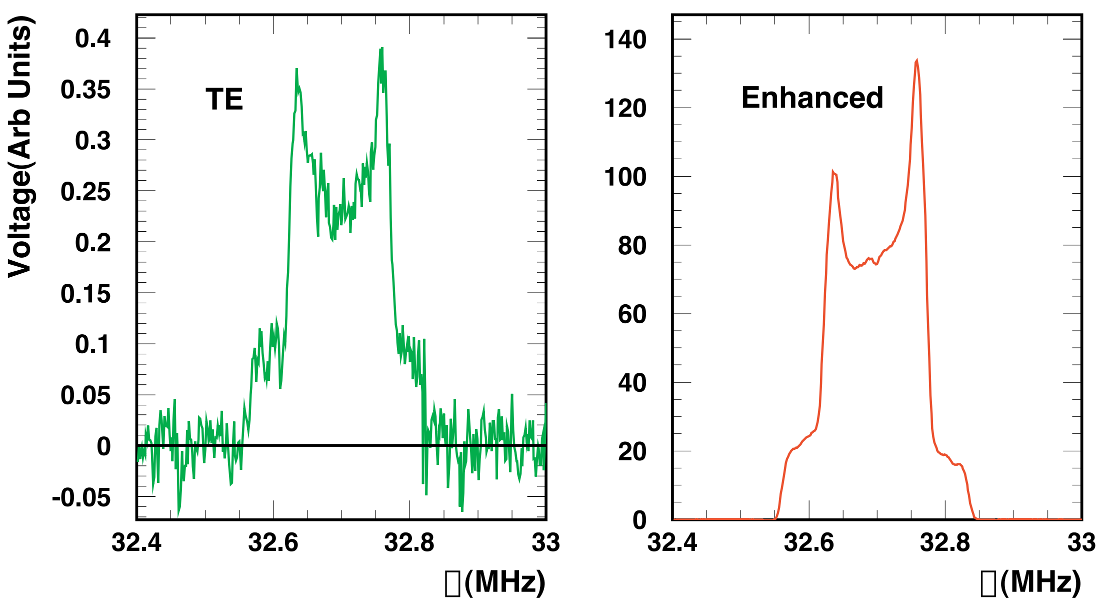

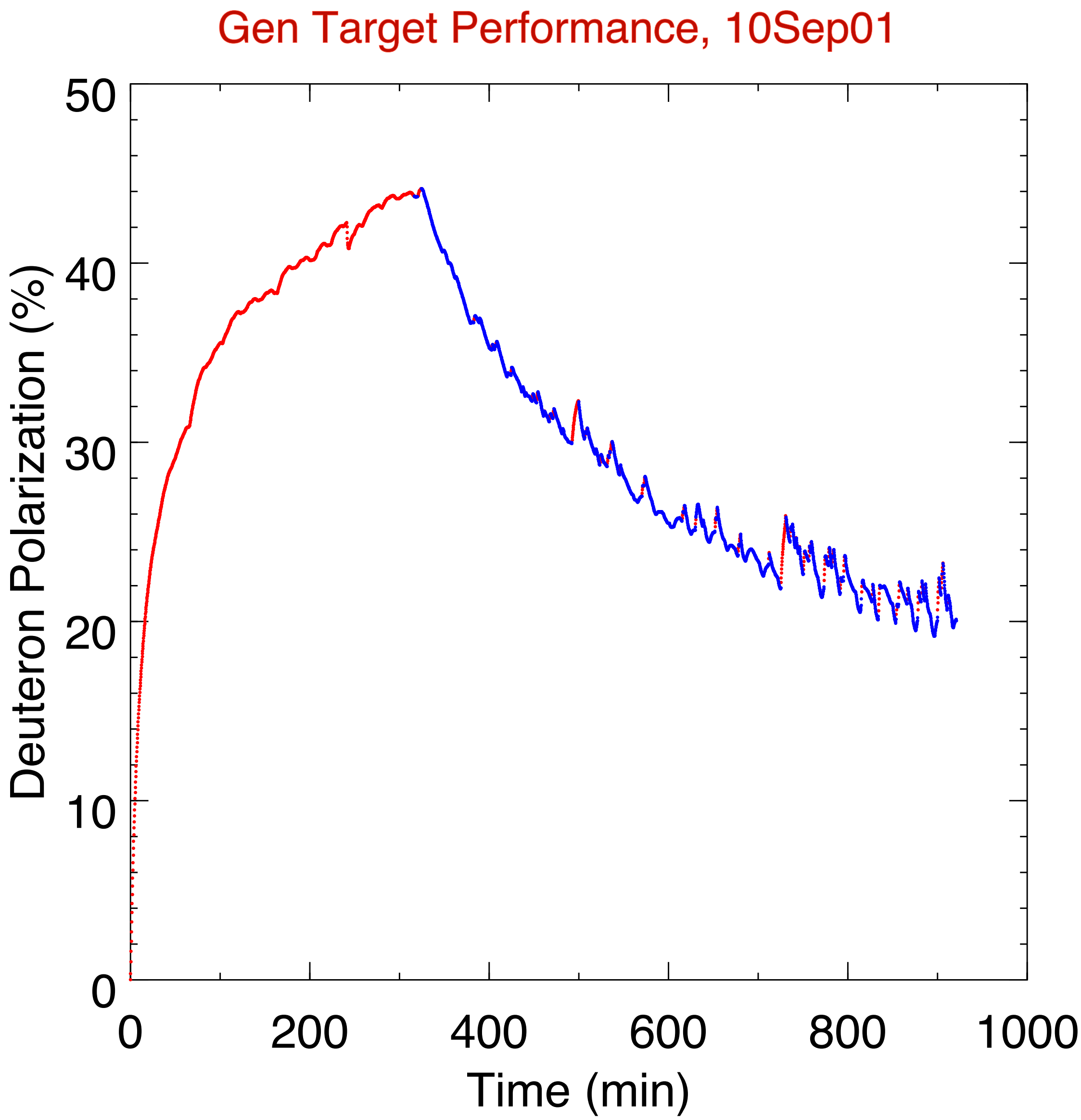

Average polarization $\simeq 25\%$

Neutron Detector

- Highly segmented scintillator
- Rates: 50 - 200 kHz per detector
- Pb shielding in front to reduce background
- 2 thin planes for particle ID (VETO)
- 6 thick conversion planes for neutron detection
- 142 elements total, $>$280 channels
- Extended front section for symmetric proton coverage
- PMTs on both ends of scintillator
- Spatial resolution $\simeq 10$ cm
- Time resolution $\simeq$ 400 ps
- Provides 3 space coordinates, time and energy

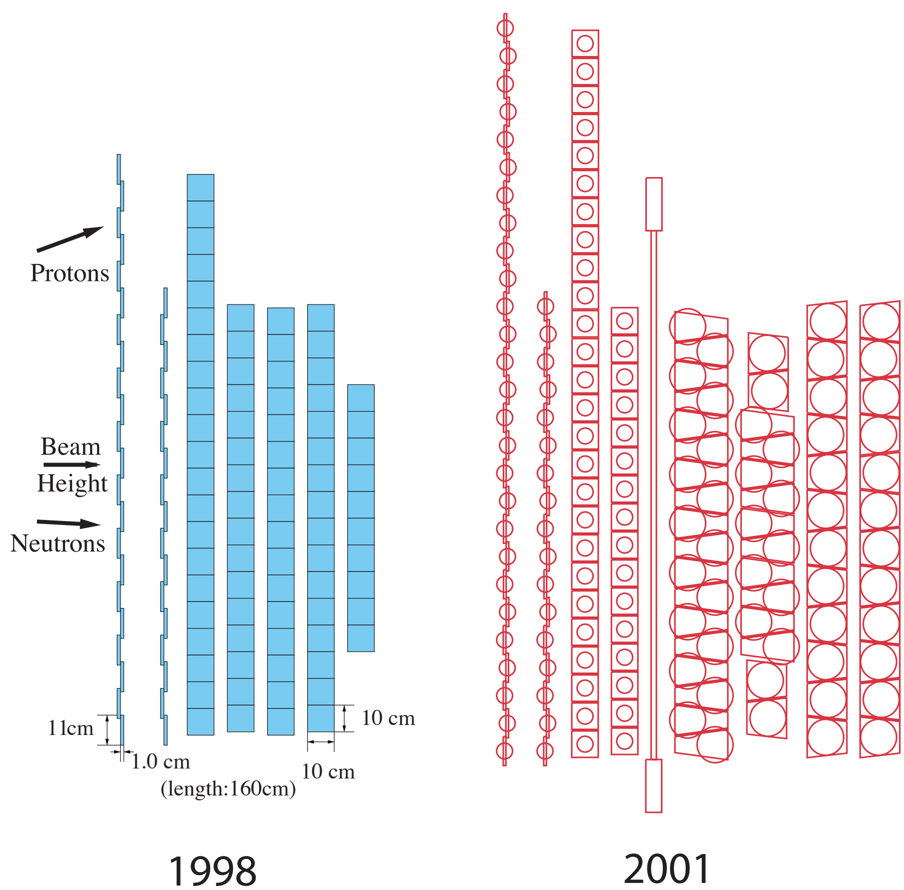


CAUTION
HIGH VOLTAGE
IN USE

Analysis

- Event Reconstruction
  - HMS standard reconstruction + target magnet + raster
  - NDET tracking: Particle Identification

$\Rightarrow$ cut variables: W, Y_{pos}, `coincidence-time`, θ_{nq}

- Event Selection and Normalization
  $\longrightarrow$ Normalized yields: $N^{\uparrow}$, $N^{\downarrow}$
- Experimental asymmetries:
  $\varepsilon = \frac{N^{\uparrow}-N^{\downarrow}}{N^{\uparrow}+N^{\downarrow}} = P_B \cdot P_T \cdot f \cdot A^V_{ed} \Rightarrow \left(A^V_{ed}\right)_{meas}$

  Dilution factor $f = \frac{N_{polarized}}{N}$ from ^{12}C
- Radiative corrections, Accidental background subtraction

$\Rightarrow$ measured deuteron asymmetry A^V_{ed} binned in four variables

- Theoretical calculations of A^V_{ed} (for different $G^n_E = \alpha \times \mathrm{Galster}$) from Arenhövel for a kinematical grid
- Average theoretical A^V_{ed} over experimental acceptance using MC and compare with measured $\left(A^V_{ed}\right)_{meas}$

$\Rightarrow G^n_E$

Timing

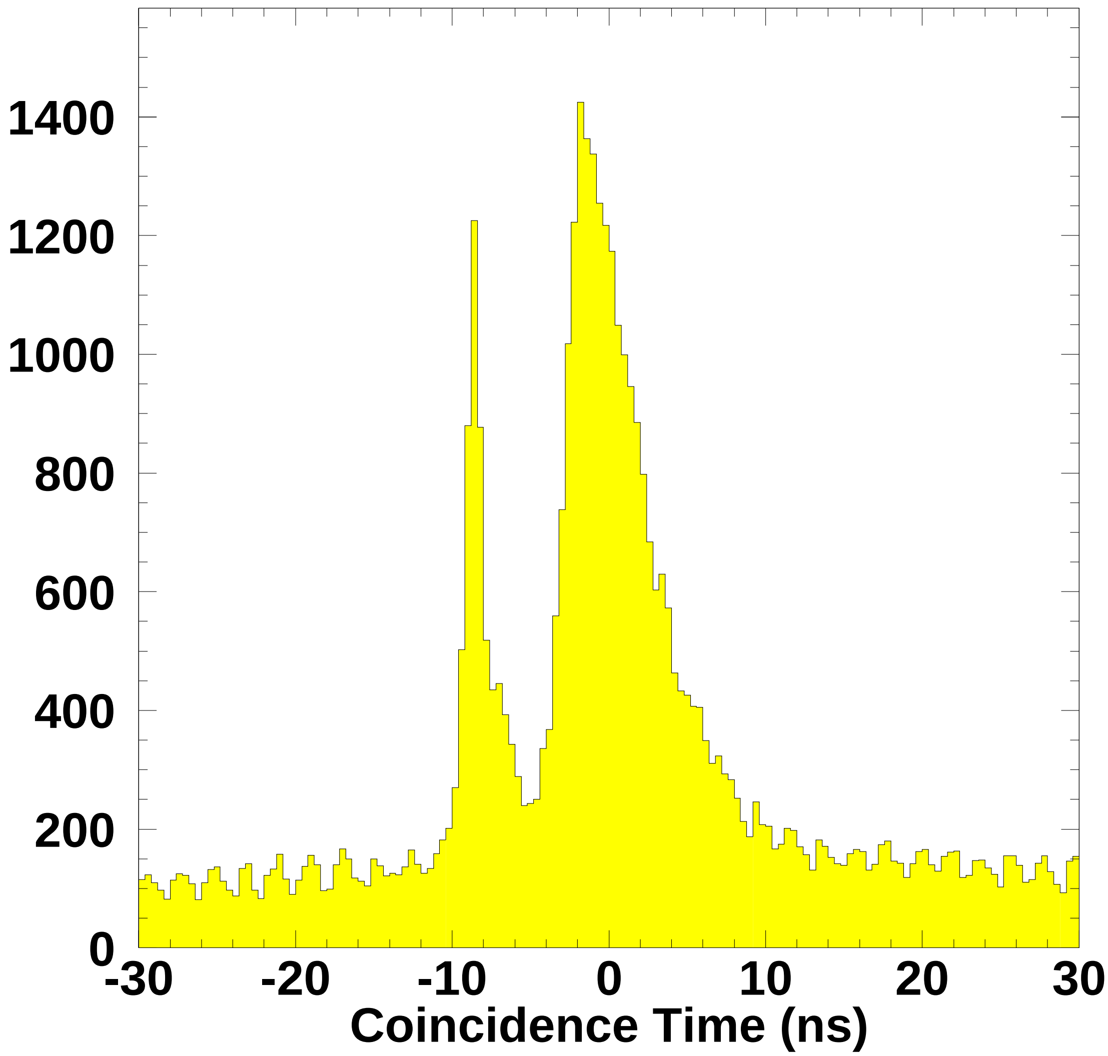
1400
1200
1000
800
600
400
200
0
-30
-20
-10
0
10
20
30
Coincidence Time (ns)

Particle Identification

- Neutrons No paddle hits along trajectory to target
- Veto inefficiency from 2/3 using first bar layer 3% per plane
- Target Field helps, $\theta_{nq} < 0.1$ rad
- Protons bent $\approx$ 17 deg (0.3 rad)

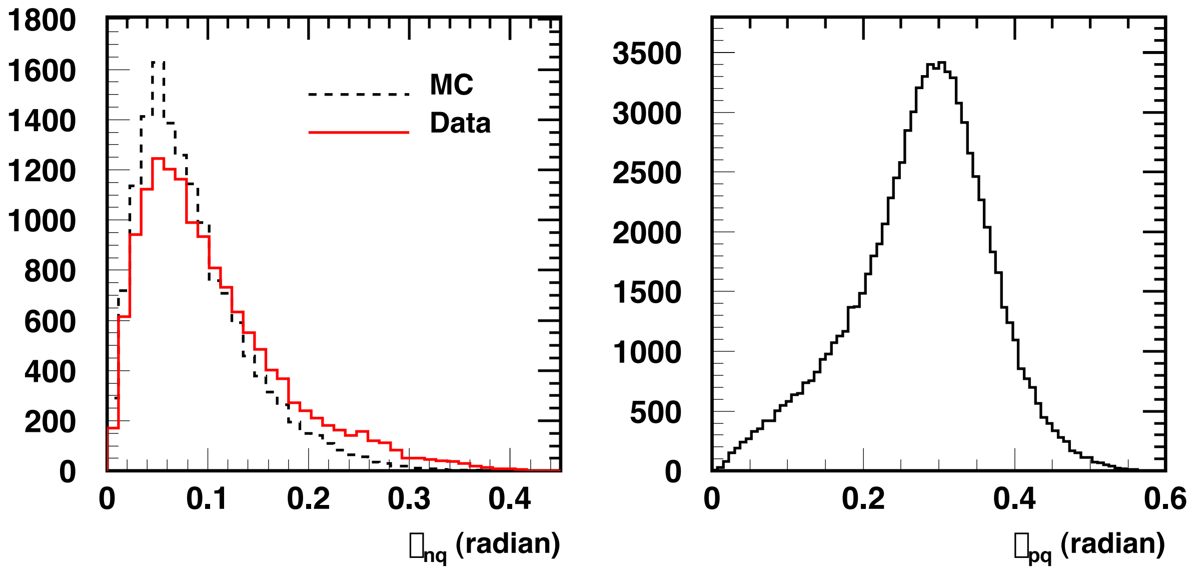

Particle Identification

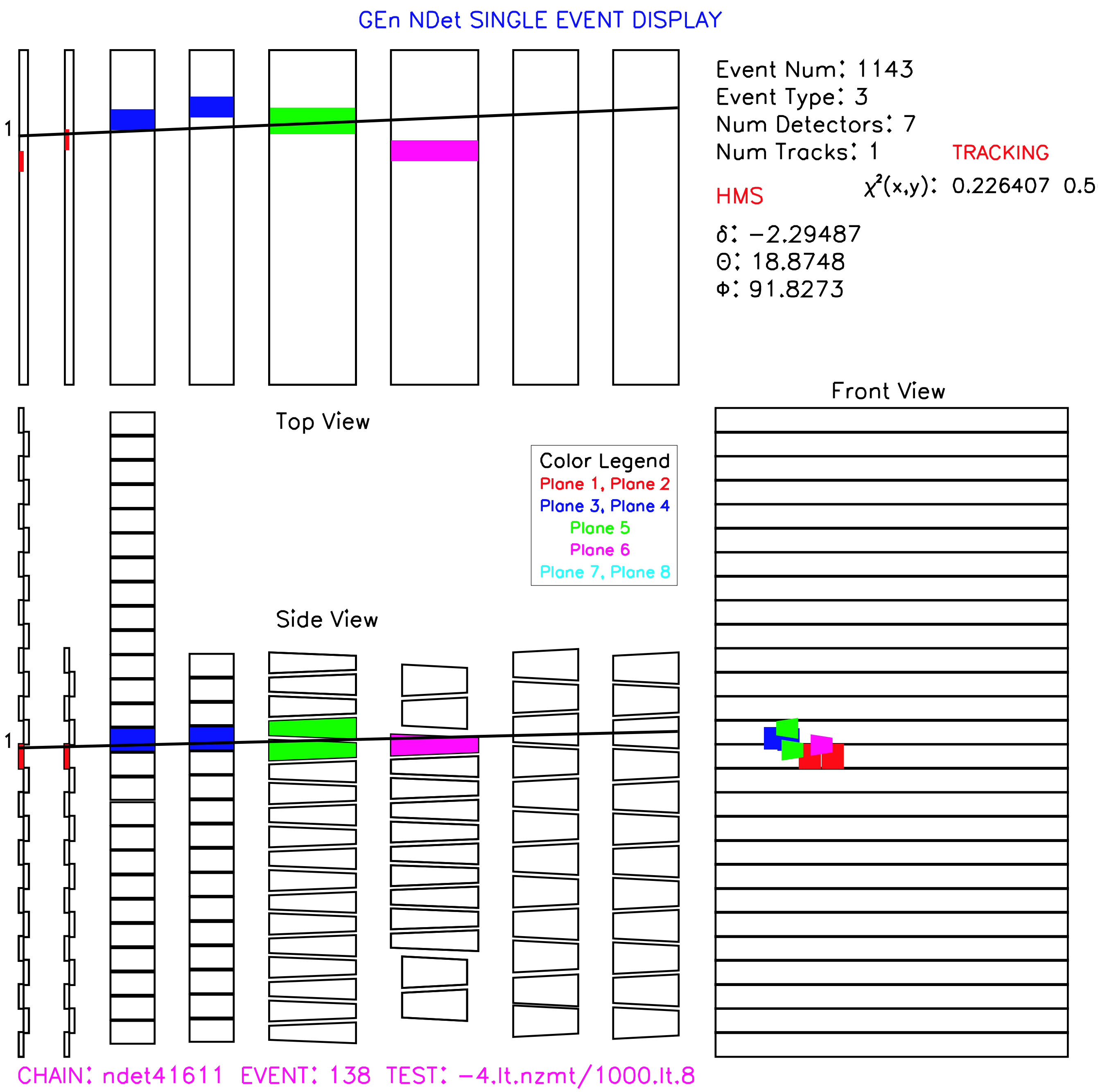

Not typical–most protons above the bulk of the bars

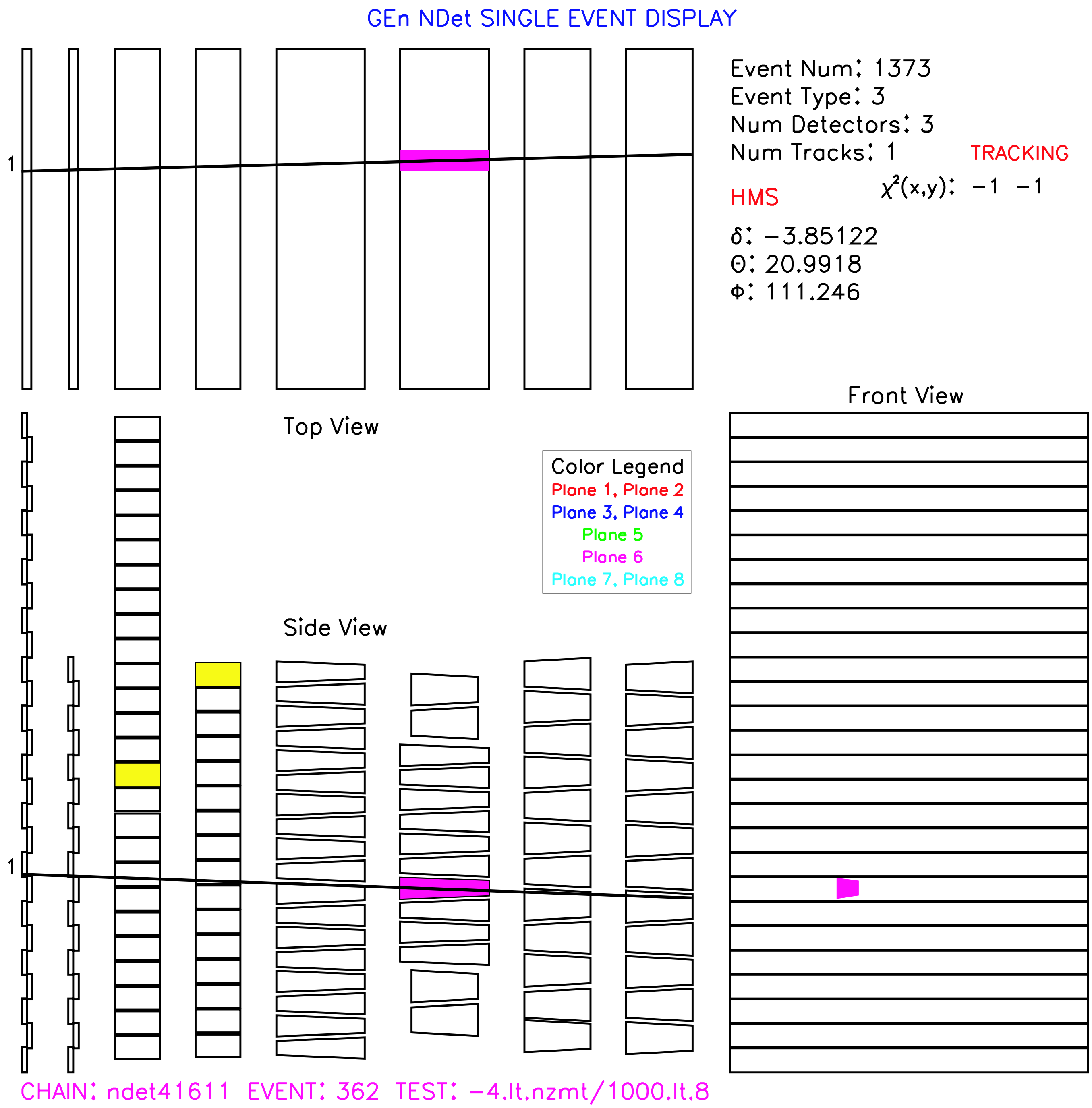

Fired but failed the MT cut.

Experimental Asymmetries

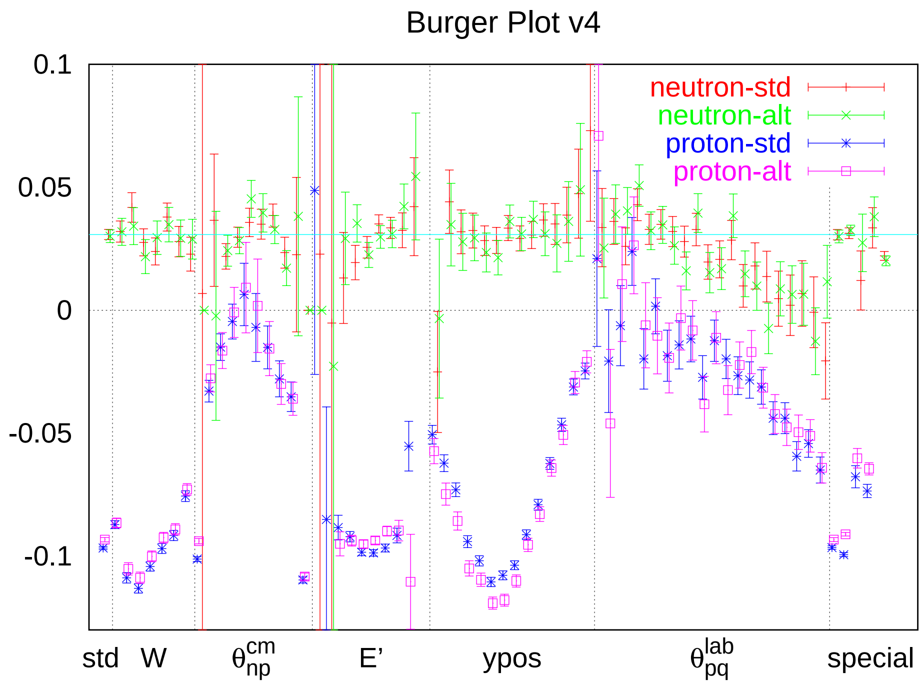

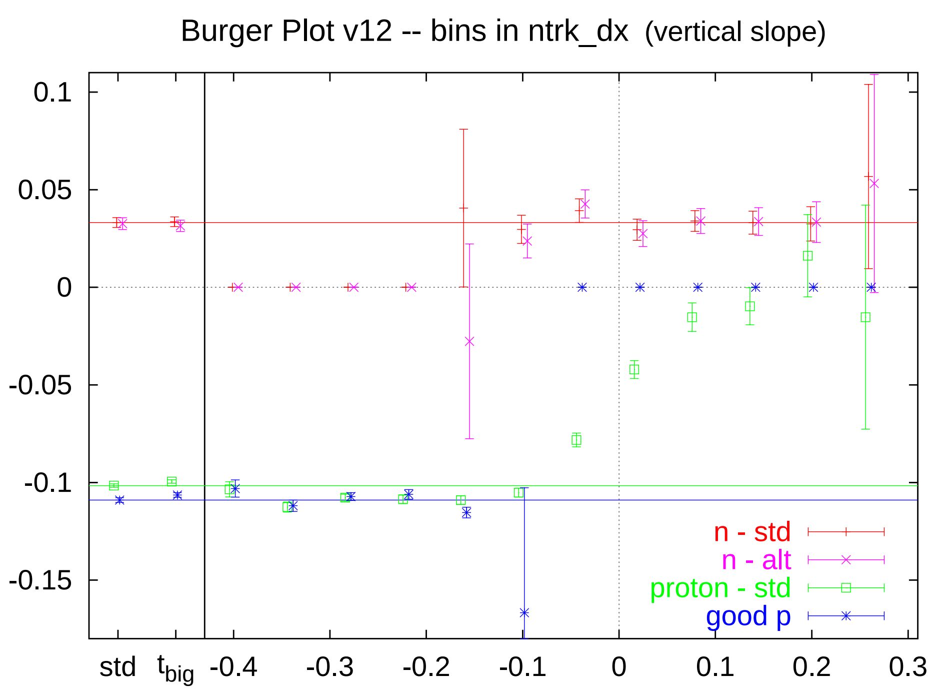

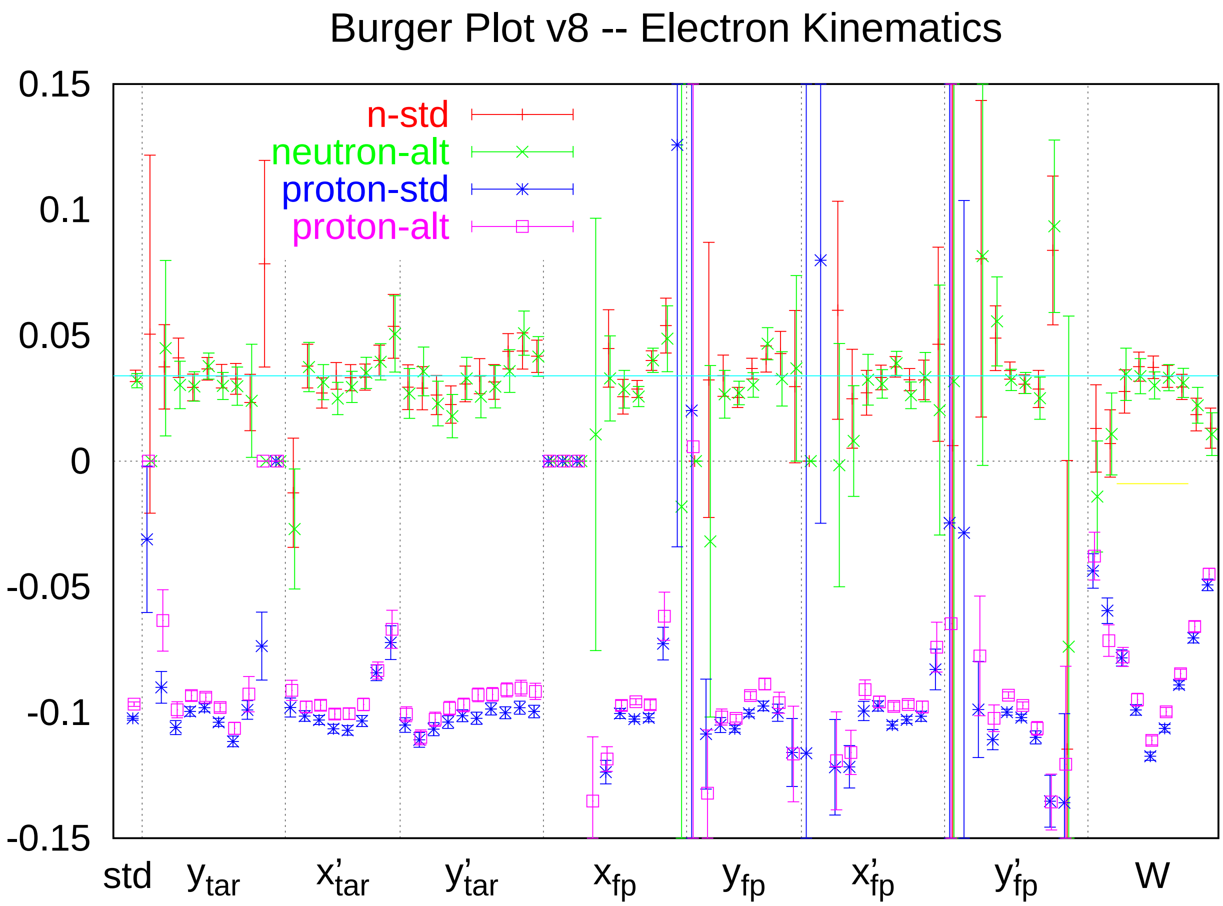
Burger Plot v8 -- Electron Kinematics
n-std
neutron-alt
proton-std
proton-alt
0.15
0.1
0.05
0
-0.05
-0.1
-0.15
std
y_{tar}
x'_{tar}
y'_{tar}
x_{fp}
y_{fp}
x'_{fp}
y'_{fp}
W

Dilution factor

Solution: Monte Carlo and experimental data

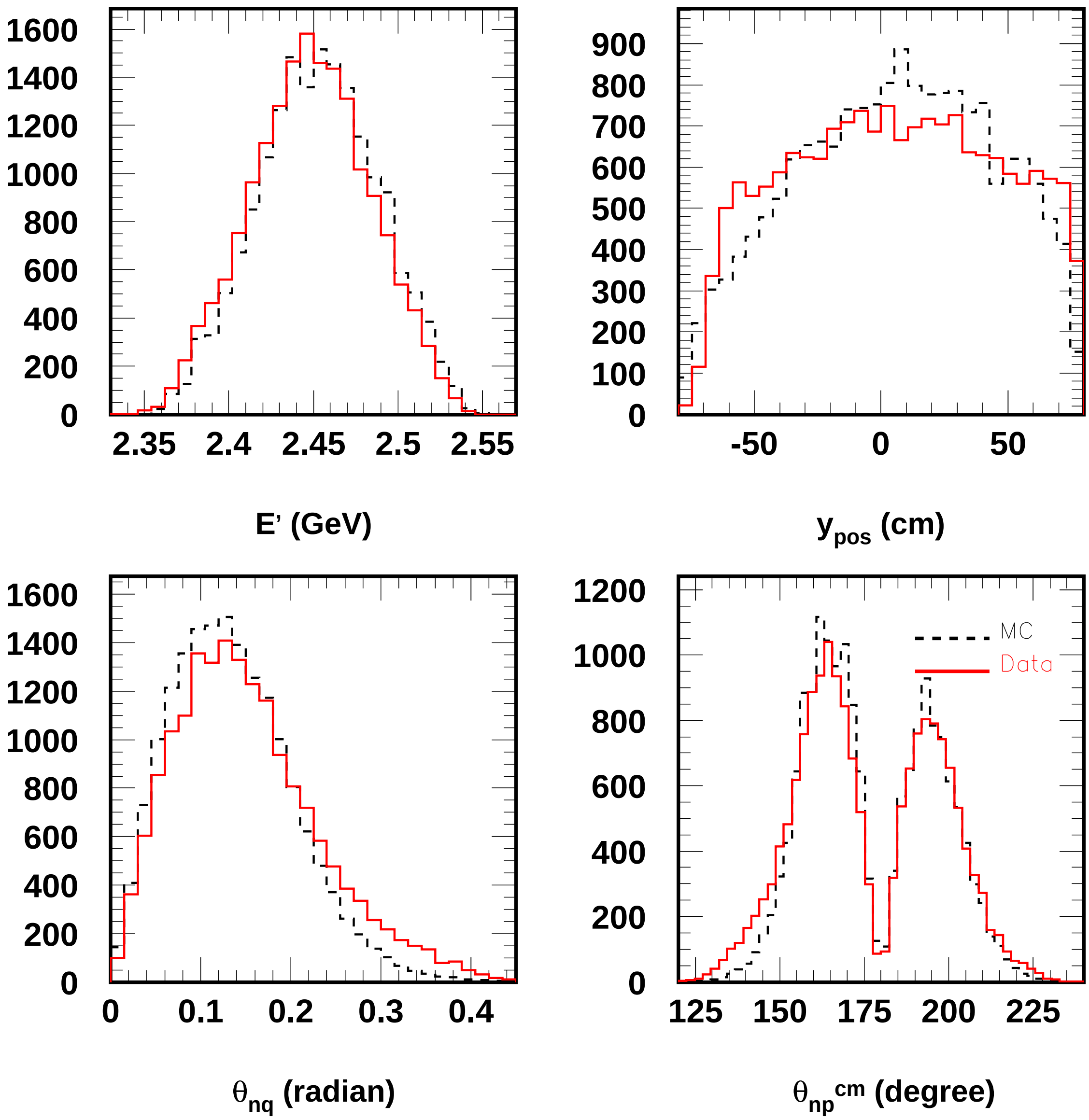

Structure of A_{ed}^{V}

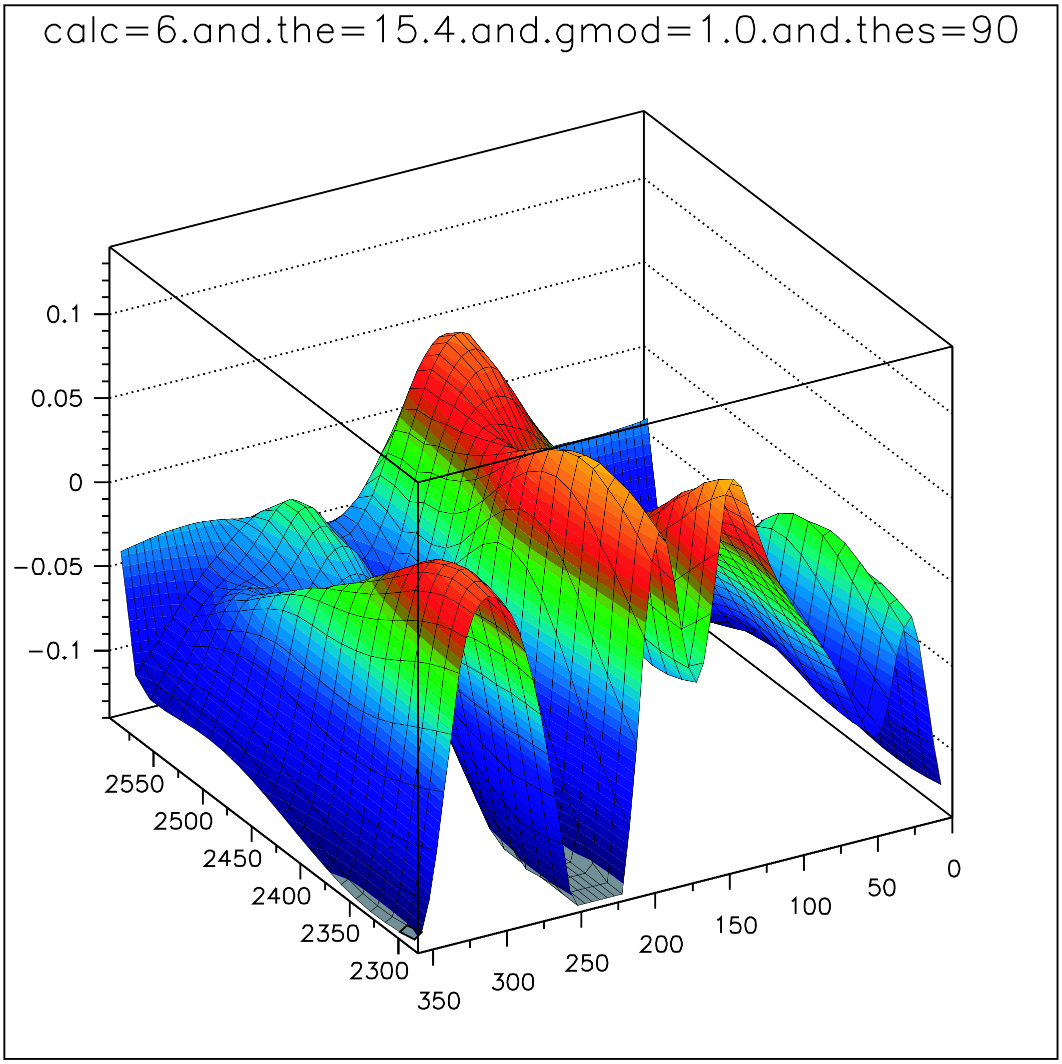

Extracting G_E^n

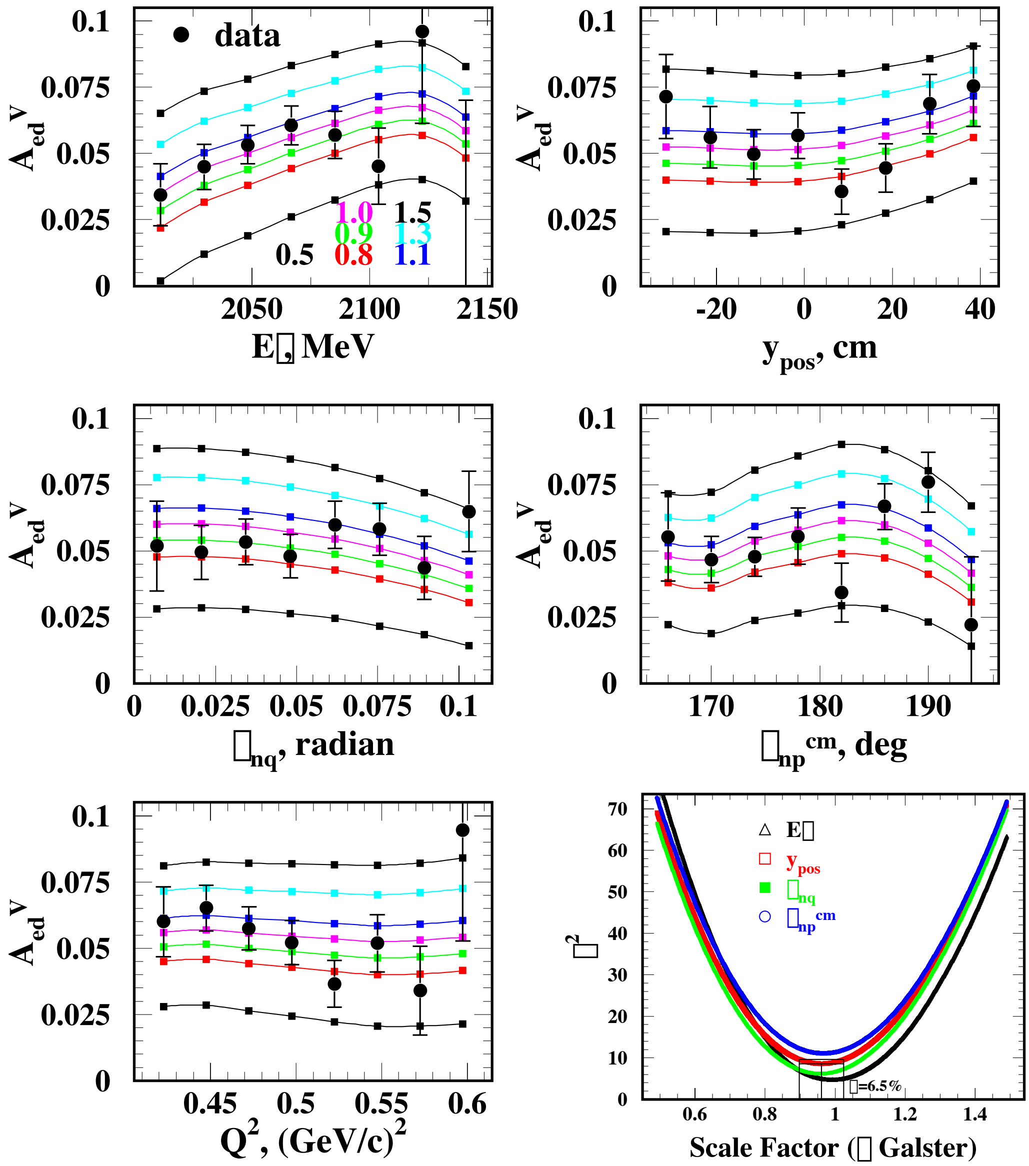

Extracting G_E^n

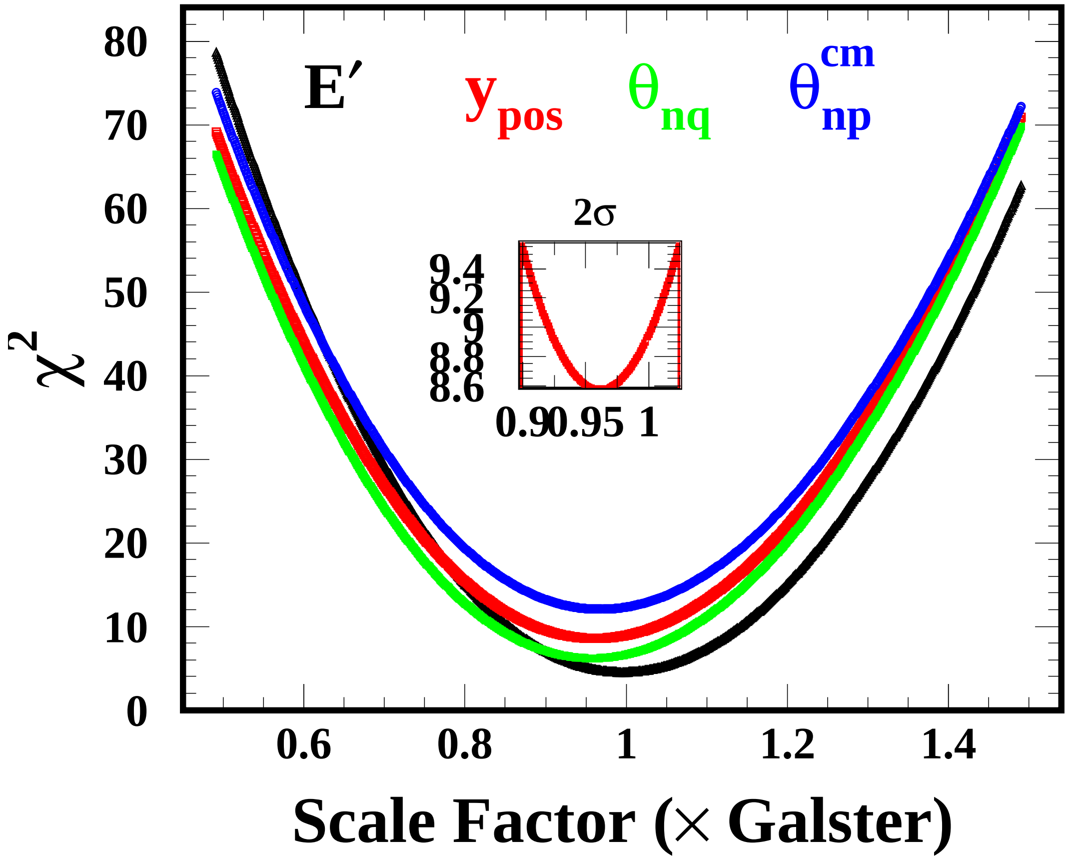

E': Energy of the scattered electron

Y_{pos}: Horizontal coordinate of the hadron track in the neutron detector

θ_{nq}: Angle between 3-momentum transfer ($\overrightarrow{q}$) and hadron track

$\theta_{np}^{\mathrm{cm}}$: Angle between neutron and ($\overrightarrow{q}$) in cm

CEX and multi step processes

Not all good neutrons are generated by quasielastic scattering. Data and asymmetry get contaminated, in the following way.

- in the lead shielding in front of the neutron detector:
  - d(e,e'p) followed by $Pb(p,n)$
  - d(e,e'p) followed by $Pb(p,\pi^0)$ and $\pi^0 \rightarrow \gamma + \gamma$
- the $^{15}\mathrm{ND}_3$ target
  - d(e,e'p) followed by ^{15}N(p,n)

First estimates of Pb(p,n) revealed that this effect is not neglible.

- A simulation was written using the measured proton distribution in the detector; Pb(p,n) cross section from charge exchange studies for G_M^n.
- The net contamination in asymmetry due to Pb(p,n) is $-3.44 \pm 1.02\%$ for $Q^2 = 0.5$. The error dominated by the uncertainty in the cross section.
- For $Q^2 = 1$ the simulation has not been run. Estimate of contamination is $-3 \pm 3\%$.
- The ^{15}N(p,n) contamination is small and is estimated to be $-0.3\% \pm 0.3\%$ for $Q^2 = 0.5$ and $Q^2 = 1$.
- Photon contamination is neglible for $Q^2 = 0.5$ and about one order of magnitude smaller than from Pb(p,n) for $Q^2 = 1$ based on total cross section of proton induced π^0 production.

Preliminary Results

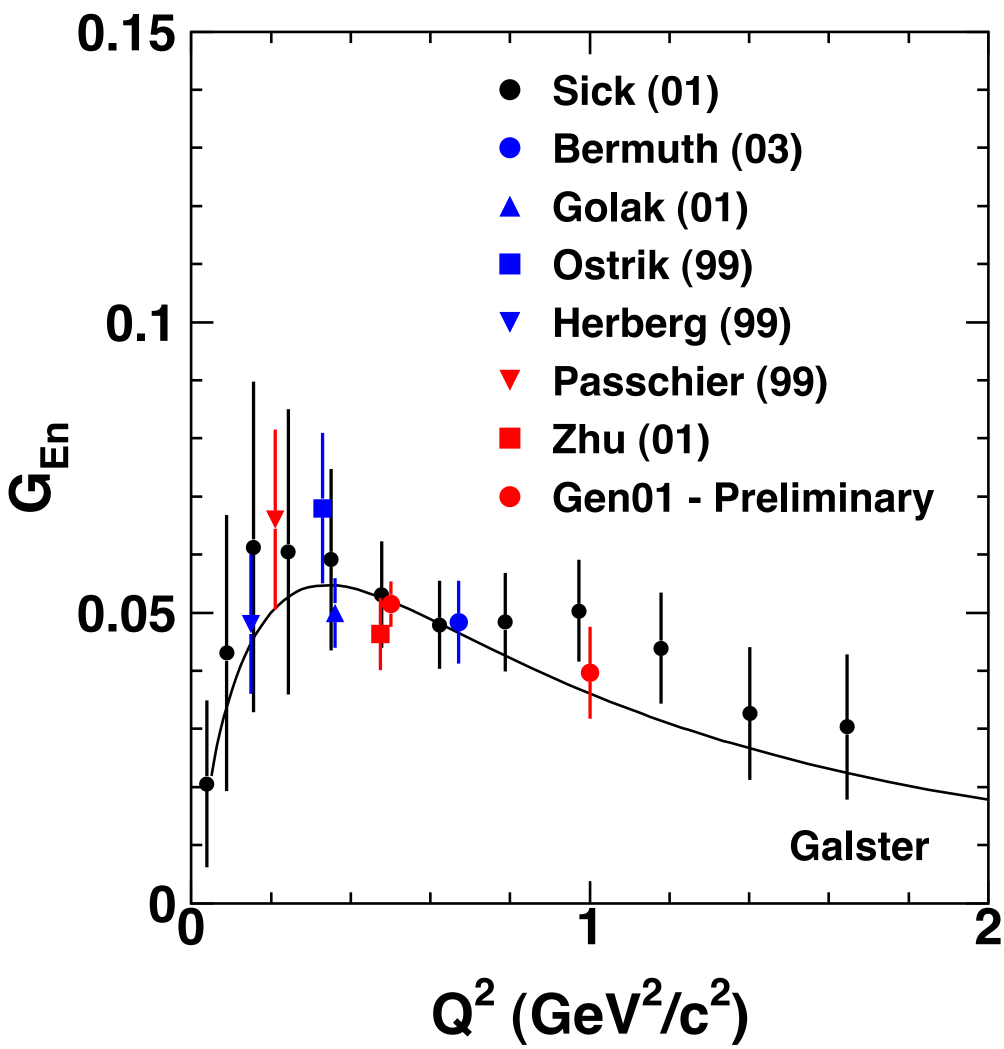

Result for 1998 $Q^2 = 0.5\,(GeV/c)^2$:

$$G_E^n = 0.04632 \pm 0.00616_{stat} \pm 0.00341_{syst}$$

⋆ *PRL 87 (2001) 081801*

Preliminary Results and Systematics

Final (98)*	$Q^2 = 0.5\,(GeV/c)^2$	$G_E^n = 0.04632 \pm 0.0070$
Preliminary (2001)	$Q^2 = 0.5\,(GeV/c)^2$	$G_E^n = \simeq \text{Galster} \pm \simeq 7.5\%(\text{stat.})$
Preliminary (2001)	$Q^2 = 1.0\,(GeV/c)^2$	$G_E^n = \gtrsim \text{Galster} \pm \simeq 14\%(\text{stat.})$

Systematics	98	01 (predicted)
Target Polarization	5.8%	3-5%
Dilution Factor	3.9%	3%
Cut Dependence	2.4%	2%
Kinematics	2.2%	2%
G_M^n	1.7%	1.7%
Beam Polarization	1.0%	1-3%
Other	1.0%	1%
Sum	8.0%	6-8%

Comparison to Models

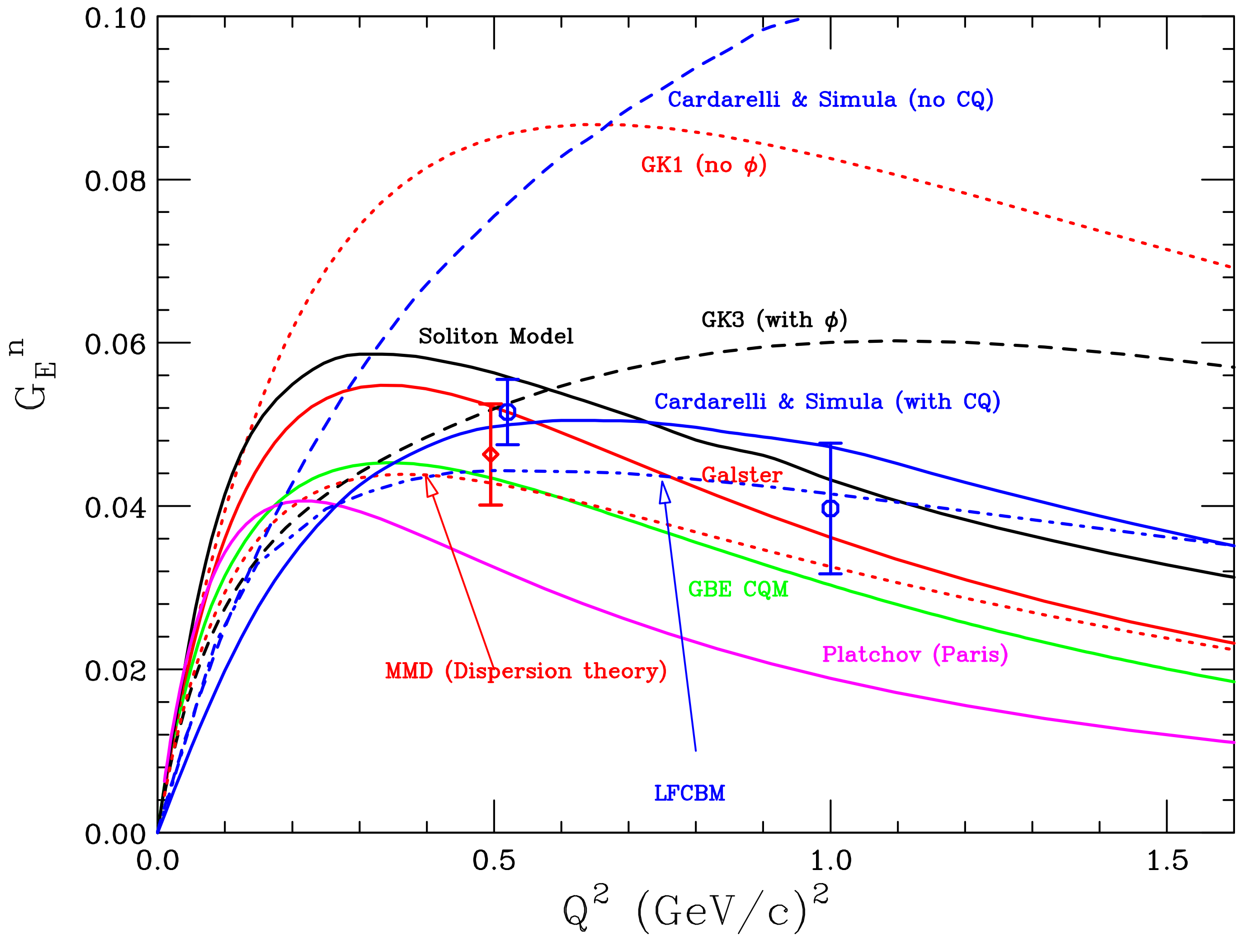

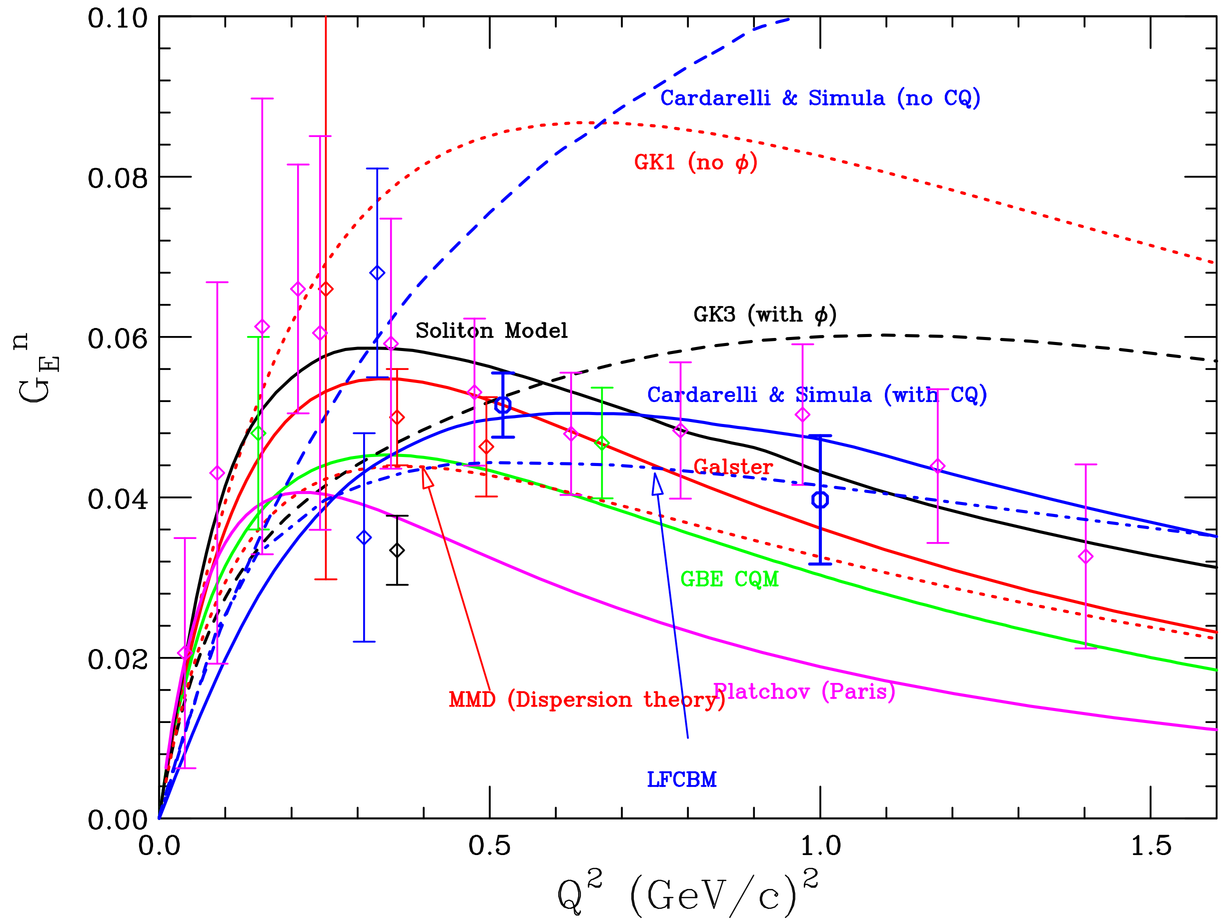

0.10
0.08
0.06
0.04
0.02
0.00
0.0
0.5
1.0
1.5
G_E^n
Q^2 (GeV/c)^2
Cardarelli & Simula (no CQ)
GK1 (no ϕ)
GK3 (with ϕ)
Soliton Model
Cardarelli & Simula (with CQ)
Galster
GBE CQM
MMD (Dispersion theory)
Platchov (Paris)
LFCBM

Comparison to Models

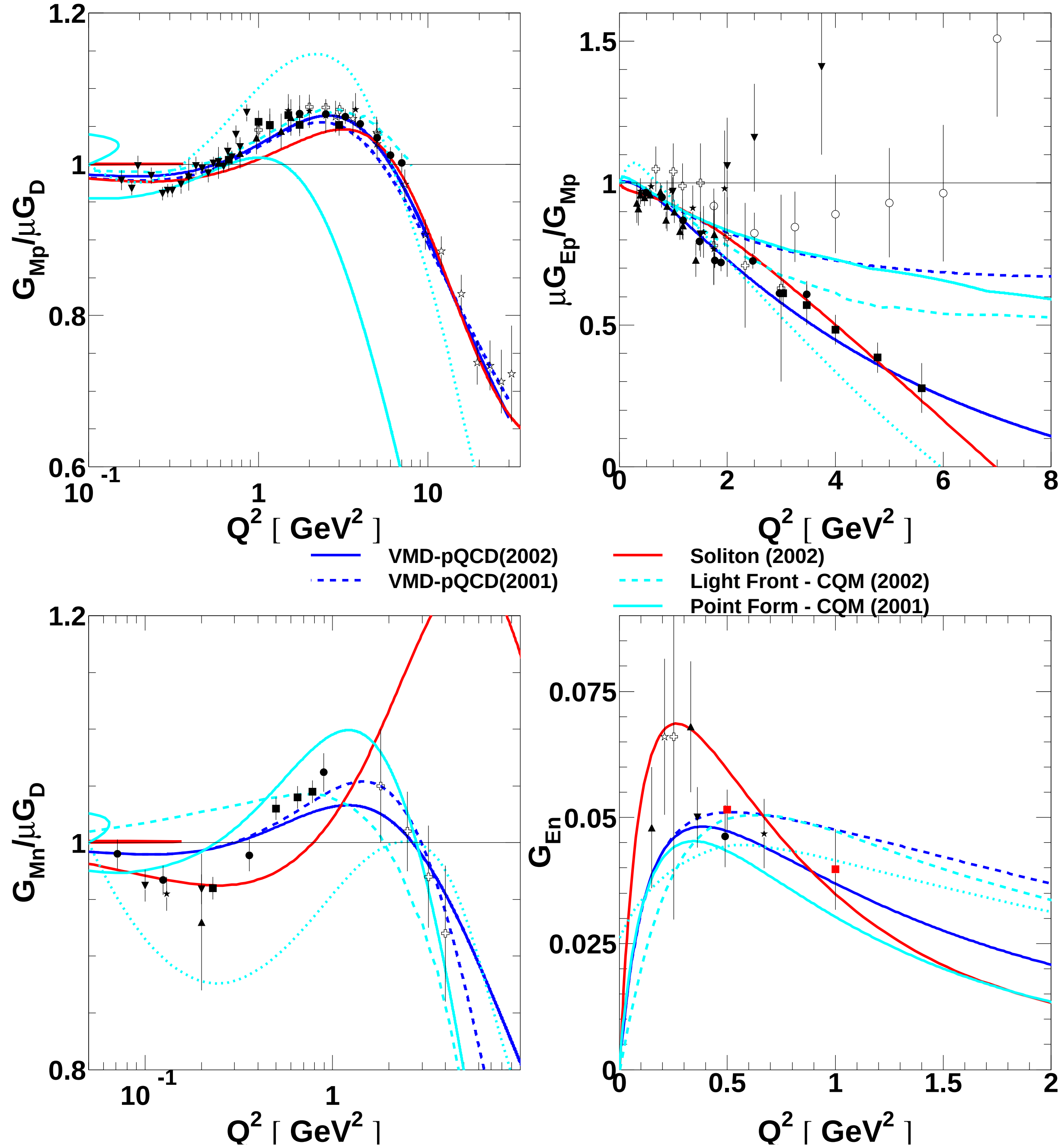

Future G_E^n Results/ Measurements

Under Analysis

- Jefferson Lab: ${}^2\overrightarrow{\mathrm{H}}(\vec{e},e'n)p$ at $Q^2 =$ 0.5 and 1.0 (GeV/c)^2 (E93026)

- Jefferson Lab: $D(\vec{e},e'\vec{n})p$ at $Q^2 =$ 0.45, 1.1 and 1.45 (GeV/c)^2 (E93038)

- Mainz: $D(\vec{e},e'\vec{n})p$ at $Q^2 =\simeq$ 0.3, 0.6 and 0.8 (GeV/c)^2

Future measurements

- Jefferson Lab: ${}^3\overrightarrow{\mathrm{He}}(\vec{e},e'n)pp$ up to at $Q^2 =$ 3.4 (GeV/c)^2

- Bates: ${}^2\overrightarrow{\mathrm{H}}(\vec{e},e'n)p$ and ${}^3\overrightarrow{\mathrm{He}}(\vec{e},e'n)pp$ precision measurements up to $Q^2 \simeq 1$ (GeV/c)^2 with internal targets and BLAST.

- out to 14 (GeV/c)^2 with an upgraded CLAS and the 12 GeV upgrade.

Summary

- G_E^n is related to the charge distribution of the neutron.
- G_E^n remains the poorest known of the four nucleon form factors.
- G_E^n is a fundamental quantity of continued interest.
- We extracted G_E^n from beam-target asymmetry measurements.
- G_E^n can be described by the Galster parametrization (surprisingly) and data under analysis is of sufficient quality to test QCD inspired models.
- Future progress likely with new experiments and better theory.

Reaction Mechanism Dependence

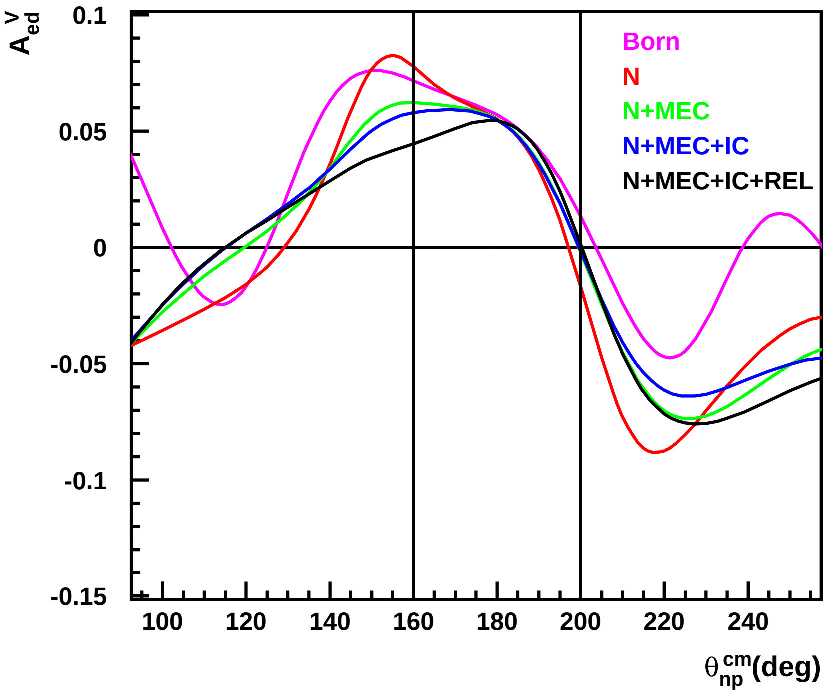

Experimental acceptance: $160\,\mathrm{deg} < \theta_{np}^{cm} < 180\,\mathrm{deg}$

Difference between full Calculation and
Born + REL: $\simeq$8%

From ε to G_E^n in Detail

The polarized beam and target electron deuteron cross section can be expressed in the form:

$$S(h, P_1^d, P_2^d) = S_0 \Big[1 + hA_e + P_1^d A_d^V + P_2^d A_d^T + h(P_1^d A_{ed}^V + P_2^d A_{ed}^T) \Big],$$

where A_e, A_d^V, A_d^T, A_{ed}^V, A_{ed}^T are electron asymmetry, vector and tensor target asymmetries, and electron-deuteron vector and tensor asymmetries.

Comparing with the cross section expression, one can obtain expressions for the five asymmetries:

$$A_e = \frac{1}{2hS_0}\left[S(h,0,0) - S(-h,0,0)\right],$$

$$A_d^V = \frac{1}{2P_1^d S_0}\Big[S(0,P_1^d,P_2^d) - S(0,-P_1^d,P_2^d)\Big],$$

$$A_d^T = \frac{1}{2P_2^d S_0}\Big[S(0,P_1^d,P_2^d) - S(0,-P_1^d,P_2^d) - 2S_0\Big],$$

$$A_{ed}^{V,T} = \frac{1}{4hP_{1/2}^d S_0}\Big\{\Big[S(h,P_1^d,P_2^d) - S(-h,P_1^d,P_2^d)\Big] \mp \Big[S(h,-P_1^d,P_2^d) - S(-h,-P_1^d,P_2^d)\Big]\Big\}.$$

Note that S_0 is in the denominator and we never measure S_0.

$$S(+h) + S(-h) \neq S_0$$

.

$$\varepsilon = \frac{(L_+ - R_+) - (L_- - R_-)}{(L_+ + R_+) + (L_- + R_-)}.$$

$$L_+ = \Phi_+ n_D S(h, P_1^d, P_2^d)$$
$$L_- = \Phi_- n_D S(h, -P_1^d, P_2^d)$$
$$R_+ = \Phi_+ n_D S(-h, P_1^d, P_2^d)$$
$$R_- = \Phi_- n_D S(-h, -P_1^d, P_2^d)$$

$$\varepsilon = \frac{h\left[(1-\beta)A_e + (1+\alpha\beta)P_1^d A_{ed}^V + (1-\beta\gamma)P_2^d A_{ed}^T\right]}{(1+\beta) + (1-\alpha\beta)P_1^d A_d^V + (1+\beta\gamma)P_2^d A_d^T},$$

$$\alpha = -\frac{P_{1-}}{P_{1+}}$$

$$\beta = \frac{\Phi_-}{\Phi_+}$$
$$\gamma = \frac{P_2(P_{1-})}{P_2(P_{1+})}$$
$$P_2^d = 2 - \left[4 - 3(P_1^d)^2\right]^{1/2}$$

$$A_{ed}^V = \frac{1}{h(1+\alpha\beta)P_1^d}\Bigg\{\varepsilon\left[(1+\beta) + (1-\alpha\beta)P_1^d A_d^V + (1+\beta\gamma)P_2^d A_d^T\right] - h\left[(1-\beta)A_e + (1-\beta\gamma)P_2^d A_{ed}^T\right]\Bigg\}.$$

With full ϕ acceptance A_e, A_d^V and A_{ed}^T have zero contributions.

A_d^T remains. For $P_1^d = 20\%$, $P_2^d \simeq 3\%$

with $A_d^T \approx 10^{-2} A_d^T$ can be ignored

$$A_{ed}^V = \frac{\varepsilon(1+\beta)}{h(1+\alpha\beta)P_1^d}.$$

With the dilution factor

$$A_{ed}^V = \frac{\varepsilon(1+\beta)}{h(1+\alpha\beta)P_1^d f}.$$

Gen01 Collaboration

A. Aghalaryan, A. Ahmidouch, R. Asaturyan, I. Ben-Dayan, F. Bloch, W. Boeglin, B. Boillat, H. Breuer, J. Brower, C. Carasco, M. Carl, R. Carlini, J. Cha, N. Chant, E. Christy, L. Cole, L. Coman, M. Coman, D. Crabb, S. Danagoulian, D. Day, K. Duek, J. Dunne, M. Elaasar, R. Ent, J. Farrell, R. Fatemi, D. Fawcett, H. Fenker, T. Forest, K. Garrow, A. Gasparian, I. Goussev, R. Grima, P. Gueye, M. Harvey, M. Hauger, R. Herrera, B. Hu, I. Jaegle, J. Jourdan, C. Keith, J. Kelly, C. Keppel, M. Khandaker, A. Klein, A. Klimenko, L. Kramer, B. Krusche, S. Kuhn, M. Jones, Y. Liang, J. Lichtenstadt, R. Lindgren, J. Liu, A. Lung, D. Mack, G. Maclachlan, P. Markowitz, P. McKee, D. McNulty, D. Meekins, J. Mitchell, H. Mkrtchyan, R. Nasseripour, I. Niculescu, K. Normand, B. Norum, A. Opper, E. Piasetzky, J. Pierce, M. Pitt, Y. Prok, B. Raue, J. Reinhold, J. Roche, D. Rohe, O. Rondon, D. Sacker, N. Savvinov, B. Sawatzky, M. Seely, I. Sick, N. Simicevic, C. Smith, G. Smith, M. Steinacher, S. Stepanyan, J. Stout, V. Tadevosyan, S. Tajima, L. Tang, G. Testa, R. Trojer, B. Vlahovic, B. Vulcan, K. Wang, G. Warren, S. Wells, F.R. Wesselmann, H. Woehrle, S. Wood, C. Yan, Y. Yanay, L. Yuan, J. Yun, M. Zeier, H. Zhu, B. Zihlmann

Duke University, Florida International University, Hampton University, Jefferson Lab, Louisiana Tech University, Mississippi State University, Norfolk State University, North Carolina A&T State University, Old Dominion University, Ohio University, Southern University at New Orleans, Tel Aviv University, University of Basel, University of Maryland at College Park, University of Virginia, Virginia Polytechnic Institute & State University, Vrije Universiteit of Amsterdam, Yerevan Physics Institute

Impact of G_M^n

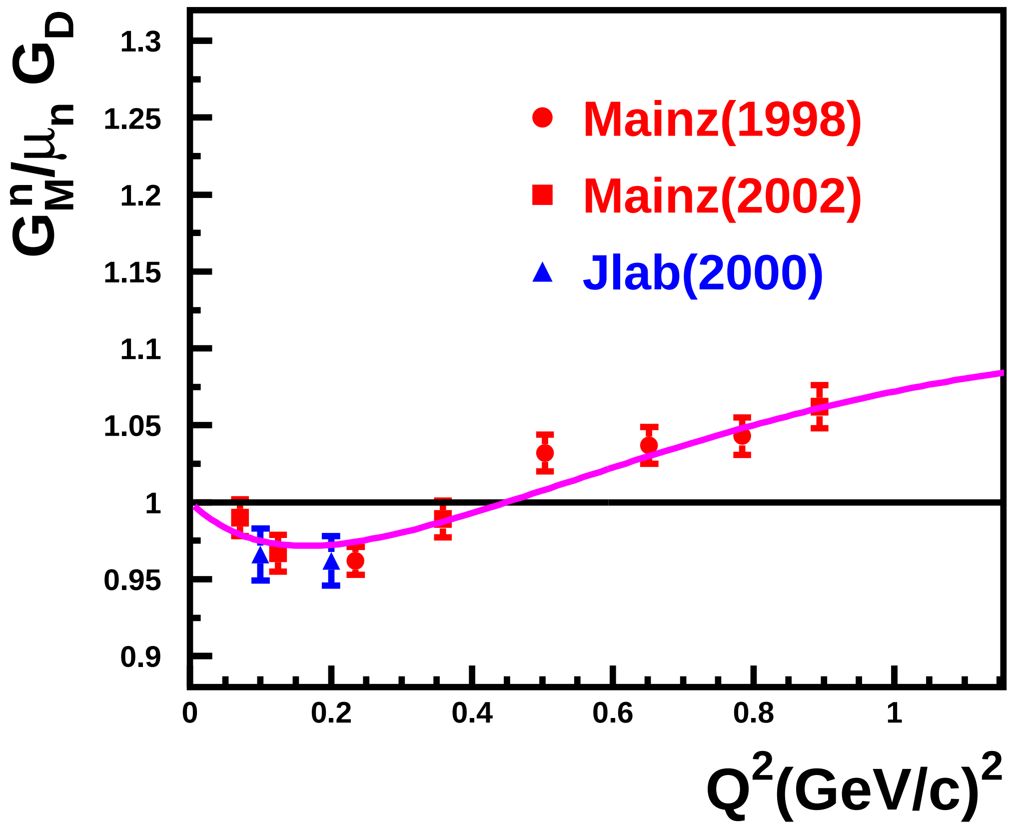

Dynamic Nuclear Polarization

Pictorial Representation–Deuteron

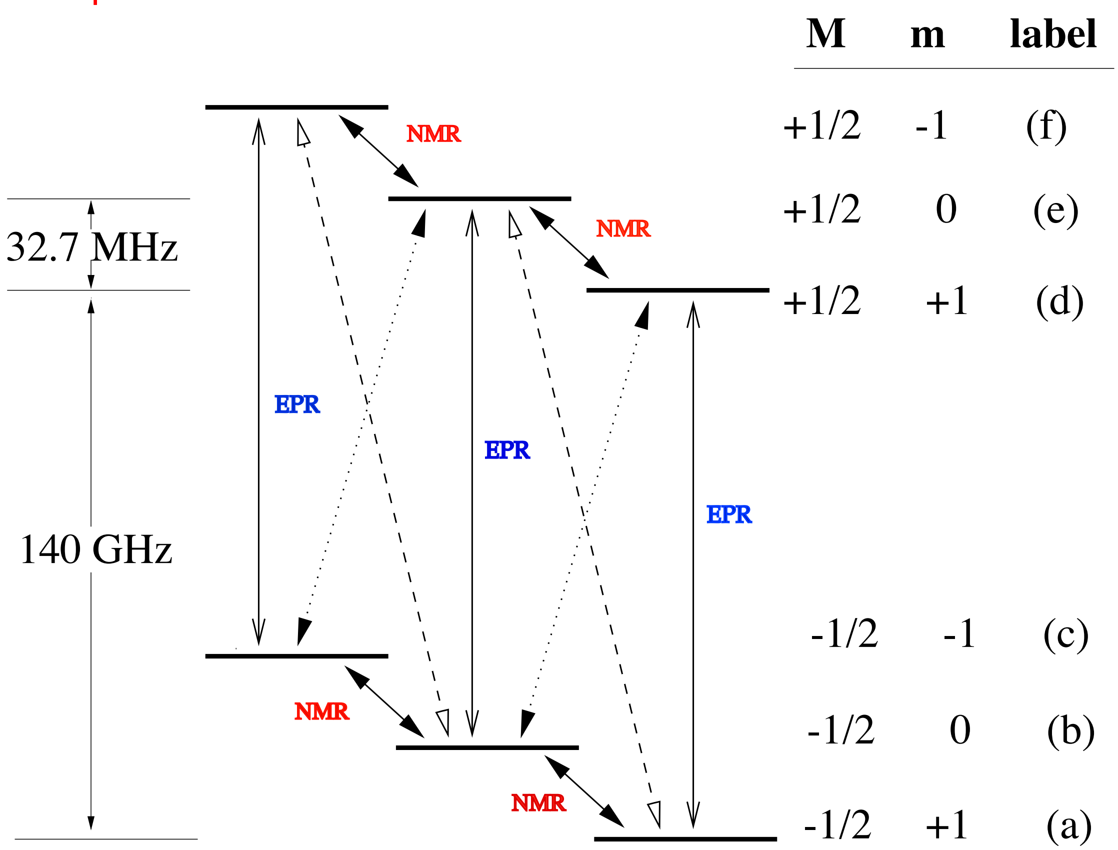

For positive enhancement drive the $\mathbf{c} \longrightarrow \mathbf{e}$ or $\mathbf{b} \longrightarrow \mathbf{d}$ transition. Relaxation occurs through $\mathbf{e} \longrightarrow \mathbf{b}$ and $\mathbf{d} \longrightarrow \mathbf{a}$ transition

NMR system

Magnetic susceptibility is a function of the frequency

$\chi(\omega) = \chi'(\omega) + i\chi''(\omega)$ consisting of a dispersive part (χ') and an absorptive part (χ'')

$P = \frac{2}{\mu_0 \pi \hbar \gamma^2 \mathrm{NJ}} \int_0^\infty \chi'' d\omega$

$L(\omega) = L_0[1 + 4\pi\eta\chi(\omega)]$

Measure the impedance of coil to get at χ''

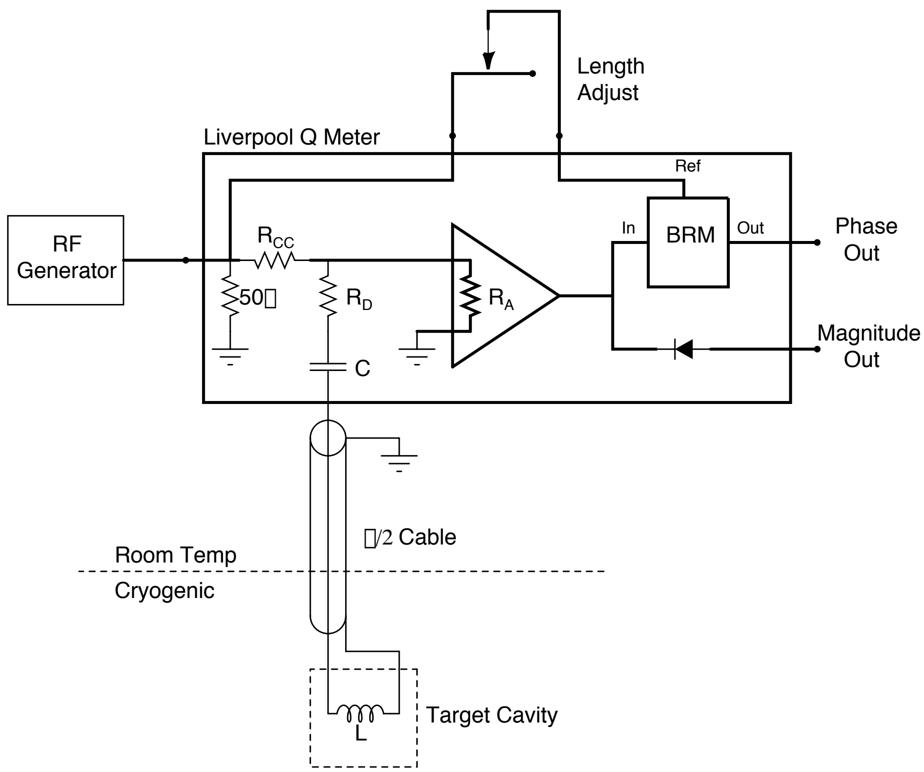

Deposited Energy-ADCs

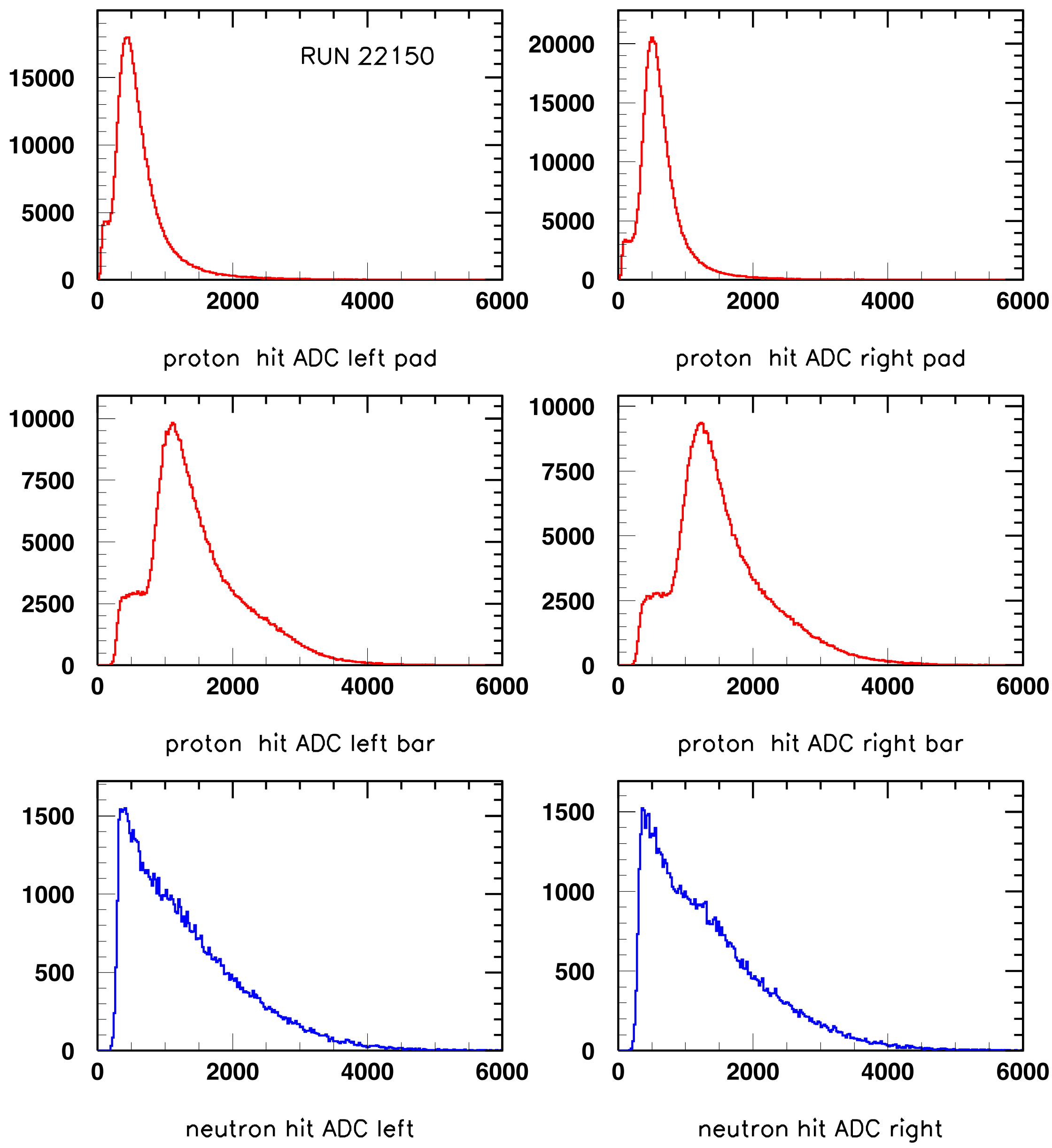

Neutrons do not have definite energy deposit due to conversion mechanism.
12-14 MeVee

Dilution Factor and Packing Fraction

$$df = \frac{R_{\text{polarized}}}{R_{\text{polarized}} + R_{\text{unpolarized}}} \qquad P_f = \frac{V_{ND_3}}{V_{\text{cell}}}$$

Material	**Source**	N_i/N_D
Nitrogen	ND_3	0.333
Helium	$(1 - P_f)$	0.240
Helium	external	0.080
Aluminum	Cell in/out	0.015
Copper	NMR Coil	0.003
Nickel	NMR Coil	0.001
**Carbon	Calibration	0.286
**Helium	Calibration	0.560

$\rho_i * \text{thickness}/A_i$

Current Asymmetry

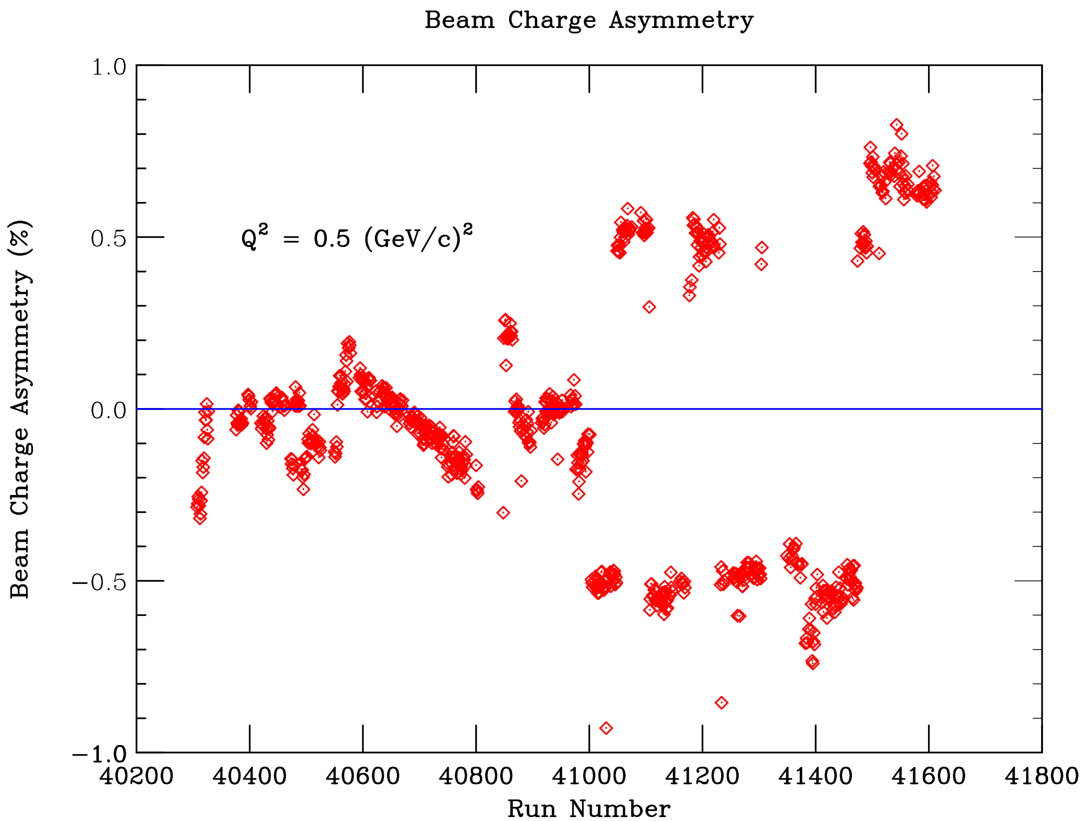

Cut Optimization

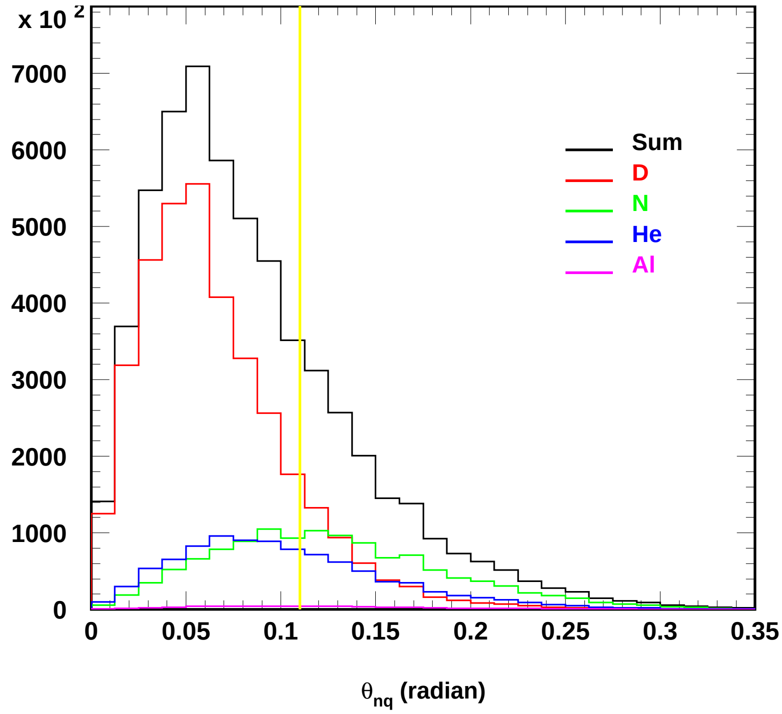

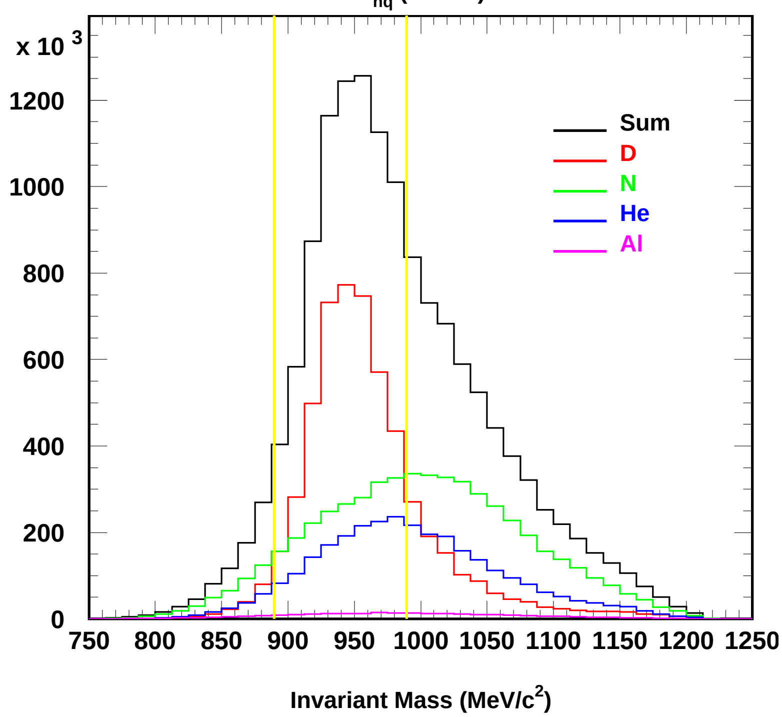

Balancing count rate and dilution factor

Accidental Background

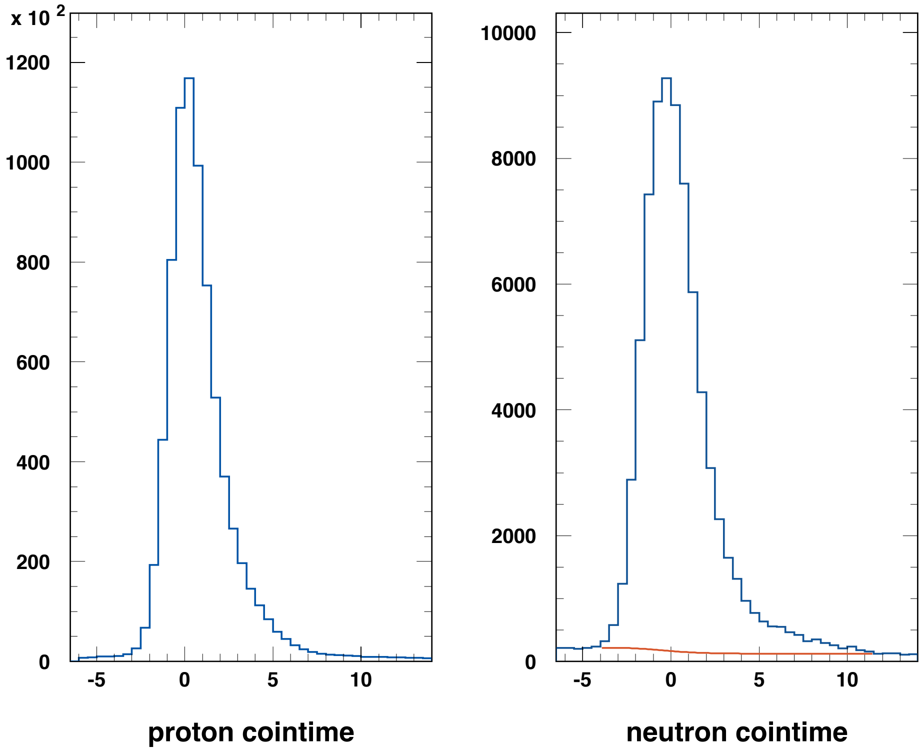

- Shape of background is determined by fact that TDC accepts only one hit
  - Randoms/Reals $\approx$ 4% for neutrons
  - Acts like dilution for unpolarized randoms

MC vs Data ND_3

Neutron

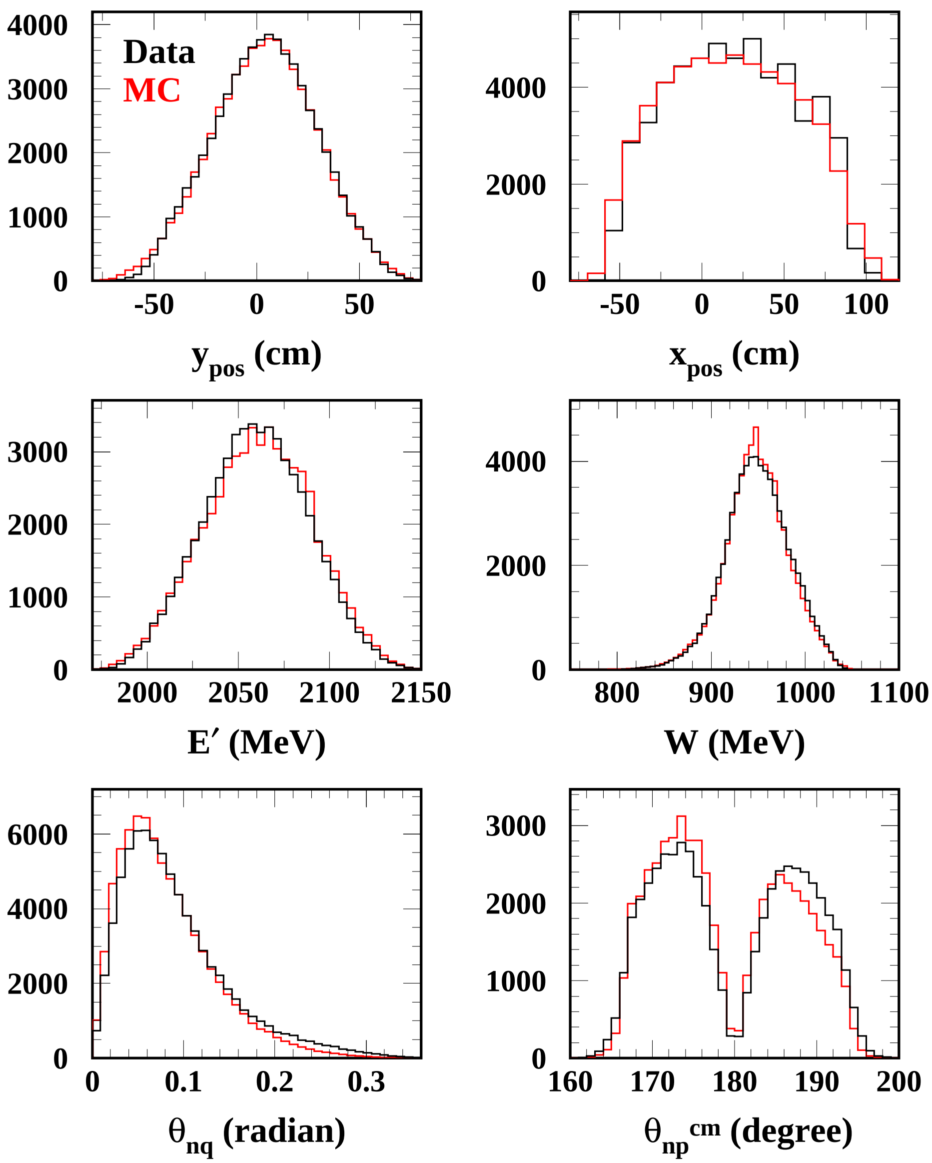

Proton

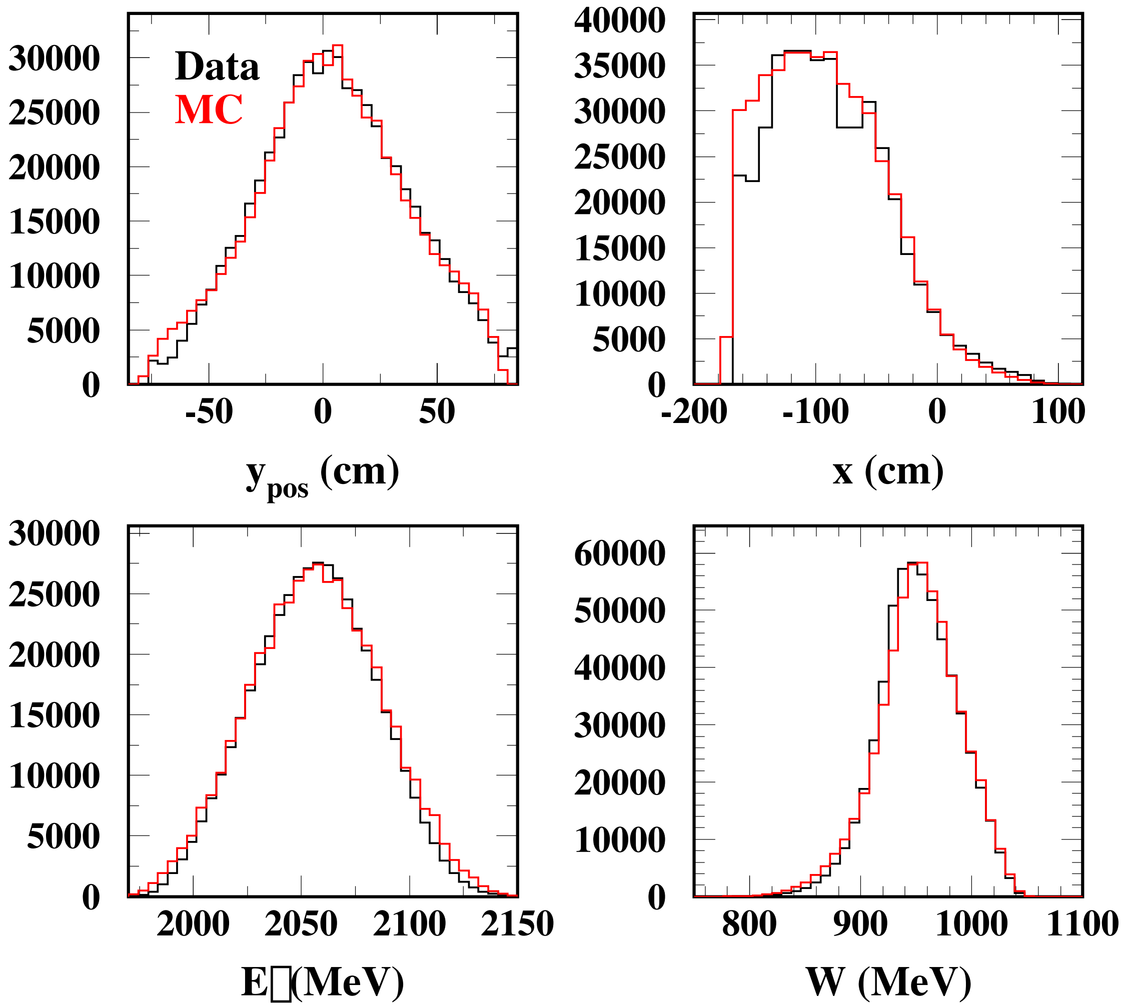

Data
MC
30000
25000
20000
15000
10000
5000
0
-50
0
50
y_{pos} (cm)
40000
35000
30000
25000
20000
15000
10000
5000
0
-200
-100
0
100
x (cm)
30000
25000
20000
15000
10000
5000
0
2000
2050
2100
2150
E (MeV)
60000
50000
40000
30000
20000
10000
0
800
900
1000
1100
W (MeV)